Fault Detection Design for Three-Phase Voltage Source Inverter in Power Train Applications

by

Lingli Gong

A thesis submitted to the
School of Graduate and Postdoctoral Studies in partial
fulfillment of the requirements for the degree of

Master Of Applied Science

Department of Electrical and Computer Engineering

University of Ontario Institute of Technology (Ontario Tech University)

Oshawa, Ontario, Canada

December 2023

THESIS EXAMINATION INFORMATION

Submitted by: **Lingli Gong**

Masters of Applied Science in **Electrical and Computer Engineering**

Thesis title: Fault Detection Design for Three-Phase Voltage Source Inverter in Power Train Applications

An oral defense of this thesis took place on November 24, 2023 in front of the following examining committee:

Examining Committee:

Chair of Examining Committee	Dr. Khalid Elgazzar
Research Supervisor	Dr. Mohamed Z. Youssef
Examining Committee Member	Dr. Walid Morsi Ibrahim
Thesis Examiner	Dr. Moustafa El-Gindy

The above committee determined that the thesis is acceptable in form and content and that a satisfactory knowledge of the field covered by the thesis was demonstrated by the candidate during an oral examination. A signed copy of the Certificate of Approval is available from the School of Graduate and Postdoctoral Studies.

ABSTRACT

This thesis is dedicated to an extensive exploration of fault detection methods tailored specifically for three-phase inverters, critical components within the propulsion systems of Electric Vehicles (EVs) and drive systems in general. A notable focal point of this study involves the application of advanced signal processing techniques to adeptly identify and diagnose potential faults. Through the signal processing mixed clustering technique, we are able to use the proposed algorithm to compare the reference gate-driving signal with the actual output voltage of the voltage source inverter (VSI) to detect the occurrences of faults. Furthermore, to facilitate this investigative journey, intricate simulation models are thoughtfully crafted utilizing the PSIM software platform. These models not only serve as practical testbeds for the proposed fault detection methods but also enable a thorough analysis and assessment of their efficacy. Some preliminary experimental results are also included to provide proof of principle.

Keywords: Fault detection; propulsion system; inverters; PSIM; power electronics.

AUTHOR'S DECLARATION

I hereby declare that this thesis consists of original work of which I have authored. This is a true copy of the thesis, including any required final revisions, as accepted by my examiners.

I authorize the University of Ontario Institute of Technology (Ontario Tech University) to lend this thesis to other institutions or individuals for the purpose of scholarly research. I further authorize University of Ontario Institute of Technology (Ontario Tech University) to reproduce this thesis by photocopying or by other means, in total or in part, at the request of other institutions or individuals for the purpose of scholarly research. I understand that my thesis will be made electronically available to the public.

Lingli Gong

Lingli Gong

STATEMENT OF CONTRIBUTIONS

This thesis primarily focuses on a comprehensive exploration of fault detection methods specifically tailored for three-phase inverters, which serve as integral components in the propulsion systems of Electric Vehicles (EVs). The work described in Chapter 2 encompasses a detailed investigation of various fault detection methodologies to enhance the reliability and safety of these critical systems. Part of this thesis is to be submitted to IEEE Transaction on Transportation Electrification to be published as:

L. Gong, and M. Z. Youssef, “Fault Detection Design for Three-Phase Voltage Source Inverter in Power Train Applications”

Part of the work in Chapter 3 has been published as:

1) L. Gong, A. Sharma, M. A. Bhuiya, H. Awad and M. Z. Youssef, "An Adaptive Fault Diagnosis of Electric Vehicles: An Artificial Intelligence Blended Signal Processing Methodology," in *IEEE Canadian Journal of Electrical and Computer Engineering*, vol. 46, no. 3, pp. 196-206, Summer 2023, doi: 10.1109/ICJECE.2023.3264852.
2) L. Gong, A. Sharma, M. Abdul Bhuiya, H. Awad and M. Z. Youssef, "An Artificial Intelligence Based Fault Monitoring of Power Trains: Design & Implementation," *2021 IEEE Applied Power Electronics Conference and Exposition (APEC)*, Phoenix, AZ, USA, 2021, pp. 2761-2768, doi: 10.1109/APEC42165.2021.9487452.
3) M. Bhuiya, L. Gong and M. Z. Youssef, "A New Multilevel Inverter Under Distributed Unbalance DC Voltage for Electric Vehicle Applications," *2021 IEEE*

Energy Conversion Congress and Exposition (ECCE), Vancouver, BC, Canada, 2021, pp. 1521-1526, doi: 10.1109/ECCE47101.2021.9595824.

I performed the majority of the synthesis, testing of membrane materials, and writing of the manuscript.

ACKNOWLEDGEMENTS

Firstly, I would like to express my gratitude to my supervisor, Dr. Mohamed Youssef. Since my undergraduate, Dr. Youssef has provided me continuous support, guidance, and understanding. I am truly grateful for all the conversations we had, and all the suggestions you shared. Secondly, I would like to thank the Ontario Tech University, for the financial support and this opportunity for me to pursue my goal. Lastly, I would like to thank my parents, my family, friends for all your encouragement support, and everlasting love.

TABLE OF CONTENTS

LIST OF TABLES

CHAPTER 1

CHAPTER 3

CHAPTER 4

LIST OF FIGURES

CHAPTER 1

CHAPTER 2

CHAPTER 3

CHAPTER 4

LIST OF ABBREVIATIONS AND SYMBOLS

EV	Electric Vehicle
VSI	Voltage Source Inverter
HMS	Health Monitor System
HV	High Voltage
EM	Electric Motor
IC	Internal Combustion
PMSM	Permanent Magnet Synchronous Machine
SOC	State of Charge
FTC	Fault-Tolerant Control
FDI	Fault Detection and Isolation
EKF	Extended Kalman Filter
IMD	Induction Motor Drives
HIL	Hardware-in-the loop
FEM	Finite Element Model
FFT	Fast-Fourier Transform
STFT	Short-Time Fourier Transform
WT	Wavelet Transform
ANN	Artificial Neural Network
DL	Deep Learning
CNN	Convolutional Neural Networks
FFN	Feed Forward Network
FDI	Fault Detection and Isolation
AC	Alternating Current
DC	Direct Current
CSI	Current Source Inverter

FOC	Field-Oriented Control
GDE	Gas Diffusion Electrode
FTC	Fault Tolerant Control
PWM	Pulse Width Modulation
SPWM	Sinusoidal Pulse with Modulation
D	Duty Cycle

Chapter 1. Introduction

1.1 Background

In year 2022, the Canadian transportation sector emitted approximately 180 million metric tons of carbon dioxide ($MtCO_2$) into the air. This marked a 7.3 percent rise compared to the emissions recorded in 2021 [1]. Development in the market of electric vehicles (EVs) is rapid to solve this globalized issue, more customers are willing to consider an electrical car instead of the gasoline vehicle. There are many advantages of the electrified automobile, mainly based on the following aspects – zero emissions, lower carbon footprint, and lower cost. The cost is lower as the maintenance requirements of electric vehicles are reduced, resulting in decreased associated maintenance expenses [2]. Table 1.1 lists the main components in a gasoline vehicle and electric vehicle, it clearly states the importance of the power converters. The complete electrical power supply system in an electric vehicle can be categorized into three stages, which are: (i) the battery charging system, (ii) the powertrain, and (iii) the regenerative braking system [3]. Figure 1.1 illustrates the architecture of the powertrain in an EV system. The electric sources, such as batteries and/or supercapacitors, are linked to the inverter via a high-voltage (HV) DC bus for the purpose of powering a high-voltage three-phase electric motor (EM) [4].

Table 1.1 Main Parts Comparison of Gasoline Vehicle and Electric Vehicle [2]

Gasoline Vehicle	Function	Electric Vehicle
Tank	Energy Storage	Battery
Pump	Energy for running the vehicle	Charger
Engine	Provides force	Electric Motor
Carburetor	Controls acceleration and speed	Controller
Alternator	Provides power	DC/DC Converter
N/A	Converts DC to AC for AC motor	DC/AC Inverter
Smog Controls	Lowers toxicity of exhaust gasses	N/A

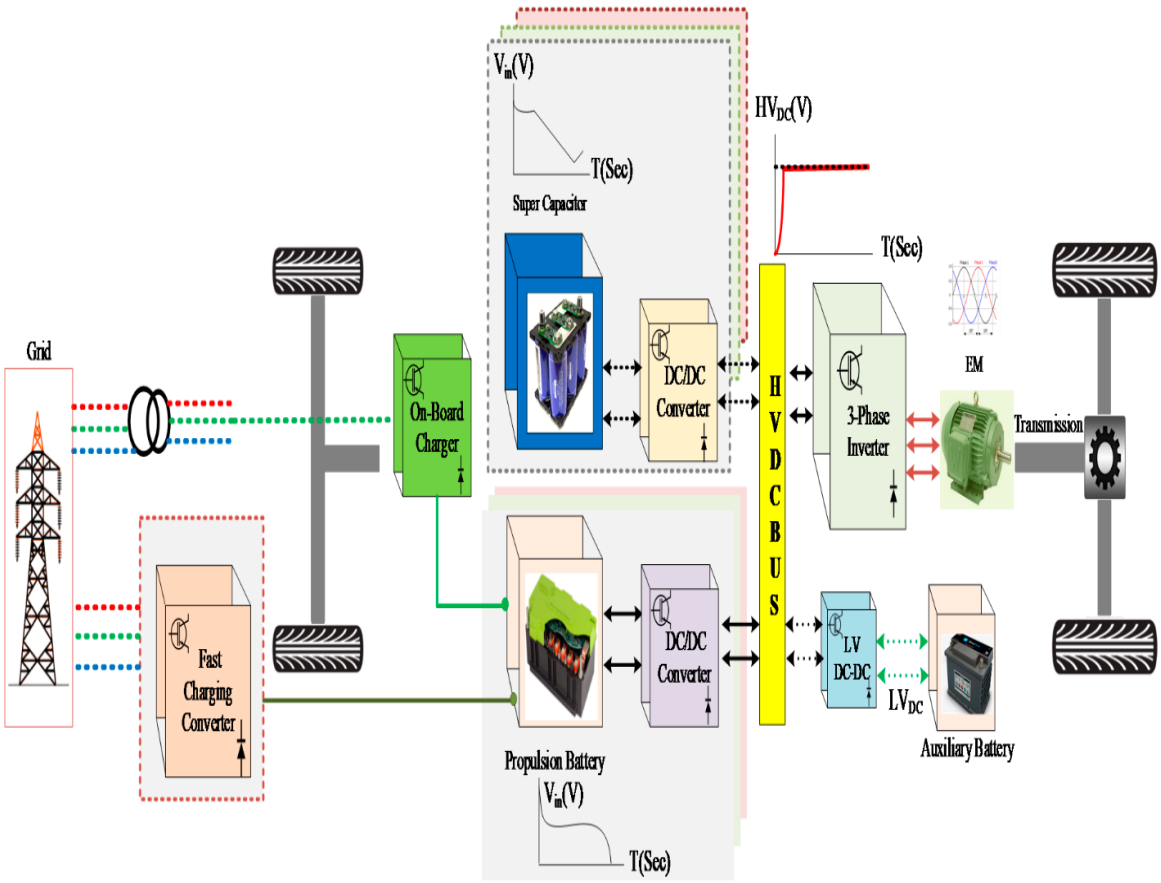

Figure 1.1 Block Diagram of The Powertrain in Electric Vehicle [4]

The core of an electric vehicle lies in its powertrain [5],[6], which consists of a battery, a traction inverter, and an electric motor. Three-phase inverters have a long history of development and are essential parts of many applications, such as electric power systems and electric cars. Nikola Tesla and George Westinghouse are the pioneers who introduced the idea of generating and distributing AC (alternating current) in the late 19th century [7]. In the 20th century, the three-phase inverter was invented and improved to adapt to various

industrial applications and designs [8]. Three-phase inverters are continuously evolving, with enhancements in efficiency, power density, and control functionalities in 21st century. The electric vehicle inverter plays a pivotal role in electric vehicles since it propels the powertrain by converting DC power from the DC-link into three-phase AC power used to drive the electric motor [3], [8]. The inverter identifies the behavior of the system similar to the Engine Management System (EMS) of combustion vehicles [8]. Figure 1.2 shows the connection topology of a three-phase inverter and an electrical system with commutation control methods.

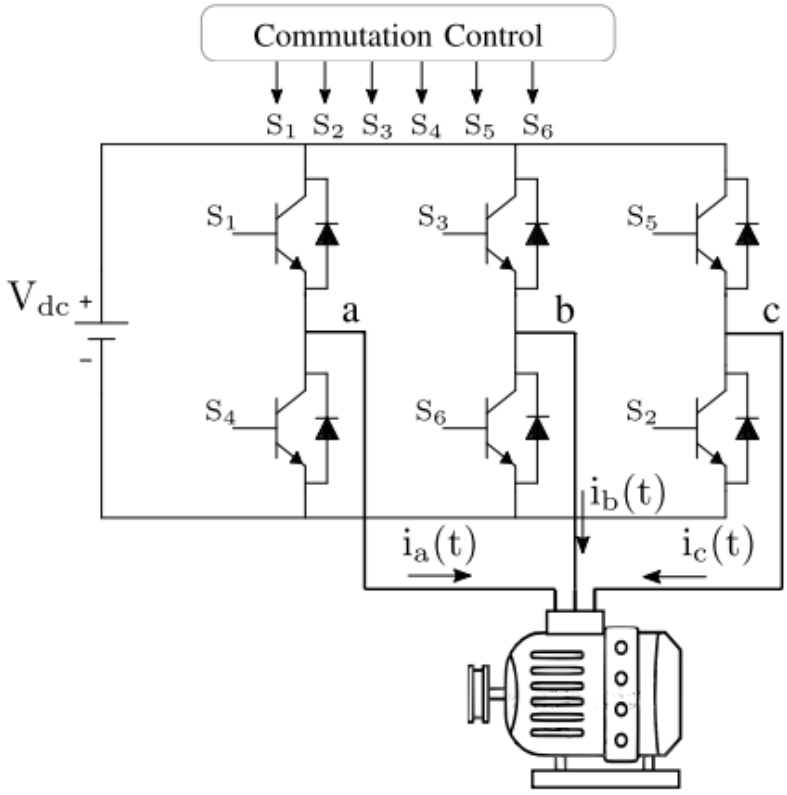

Figure 1.2 Connection of Three-Phase Inverter to An Electrical System [11]

To monitor the working condition of the inverters, it is necessary to utilize a fault detection scheme. Fault detection is employed to ascertain whether an issue has arisen within a specific channel or area of operation [9]. The main topology fault types are the short circuit fault and open circuit fault in the system. According to reports, around 38% of power inverter faults stem from malfunctioning power-semiconductor components [10]. When a short-circuit fault occurred in the electrical system, it will cause the system to cease operation. However, the open-circuit fault can cause the inverter to remain operational, potentially putting its components at risk and diminishing its performance [11]. That is to say, it is necessary to come up with a design to successfully detect an open-circuit fault appeared in the circuitry system. In this thesis, designs of open-circuit fault detection for a three-phase inverter are presented, and simulation results are presented.

1.2 Problem Statement and Motivation

Fault detection in three-phase inverters is a critical issue in various applications, including renewable energy systems, electric vehicles, industrial automation, etc. The main concern is the possibility of faults within these inverters, which can interrupt operations, cause safety hazards, and result in costly downtime and repairs. Prompt identification and resolution of these faults is critical to ensuring the reliability, efficiency and safety of their power supply systems. With the rapid growth of the electric vehicle market, and customers' concerns regards the safety, there is a need for the development of a safer and better design for the fault detection purpose. With a goal of improving the reliability and performance

of the propulsion system in the electric vehicle, the open-circuit fault detection scheme is presented.

1.3 Scope and Objective

The main objective of this thesis is to research the methodologies applicable for the fault detection in inverters. Mostly in electric vehicle applications but extends to any power train applications. Detailed modeling of the three-phase inverter and fault detection techniques will be provided in this thesis. Simulation results and analysis are also presented in this thesis report. The simulation of the design was mainly performed in the PSIM software. Preliminary experimental results are also provided.

1.4 Thesis Organization

There are five chapters in this thesis as the main body structure. The content of these five chapters can be summarized as follows:

Chapter 1 gives a general introduction of the electric vehicle and related parts. The need for such a study on the fault detection in three-phase inverter is detailed explained. This chapter also discussed the development of inverters and its fault types that could possibly occur in a circuit. This chapter also explains the problem statement and why this research was motivated. Additionally, the objectives and scope of this thesis are also discussed.

Chapter 2 is the literature review studies different approaches for fault detection, and compares the advantages and shortcomings of each technique. This chapter also presents different designs of the three-phase inverter.

Chapter 3 presents the mathematical models step by step. Relevant equations for each model are presented in this chapter.

Chapter 4 utilized all the equations listed in chapter 3 for the parameters of the components in the design. The circuit is built in PSIM environment and simulation results were obtained from PSIM software.

Chapter 5 provides a conclusion and some discussion about the future works. This chapter also includes some achievements regards this thesis.

Chapter 2. Literature Review

Electric vehicles (EVs) have emerged as a potential and ecologically friendly means of transportation in light of the urgent issues surrounding climate change and energy efficiency. EVs have garnered significant interest from consumers and businesses alike, with governments globally progressively promoting their use. As electric vehicles (EVs) increasingly permeate our everyday routines, it becomes imperative to prioritize the assurance of their safety, dependability, and performance.

The prompt highlights the need of promptly identifying and diagnosing circuit faults in the electrical and electronic systems of electric cars. Faults can occur in many components of an electric vehicle (EV), encompassing batteries, power electronics, sensors, and control systems, these have the potential to not only undermine the vehicle's operational efficiency but also pose risks to its safety and durability. It is crucial to improve the fault detection technique not only for the optimal functioning of electrical vehicles (EVs), but also for ensuring the safety of its occupants and other individuals on the sharing road.

The primary objective of this literature review is to investigate the domain of fault detection in power electronics that plays a crucial role in the EV applications. It aims to analyze the diverse approaches, technologies, and methodologies utilized for the purpose of identifying and diagnosing faults within these intricate systems. Comprehending the current advancements in fault detection has significant importance for researchers,

engineers, and policymakers, as they collaborate towards augmenting the dependability and security of electric cars.

In this section, we aim to examine the present state of defect detection in electric cars, investigate the progress made in sensor technologies, data analytics, and machine learning approaches, and evaluate the obstacles and prospects that are anticipated in this field. Through an extensive analysis of many scholarly articles, patents, and industry publications, our objective is to present a thorough and inclusive assessment of the methodologies and advancements that propel the domain of fault detection in electric cars. Through this literature, our goal is that the information we gather from this study will aid in the continuous quest to ensure that electric cars are not just sustainable, but also safe, reliable, and suitable for everyday usage.

2.1 Fault Diagnosis in Electric Vehicle Propulsion Systems

The global automotive industry has witnessed an increasing adoption of Electric Vehicles (EVs) as a result of the increased recognition of the environmental implications associated with Internal Combustion (IC) engines. The literature [12] outlines the fundamental prerequisites of an electric vehicle (EV) propulsion system, with a particular emphasis on its ability to operate efficiently and reliably in diverse operating situations, including challenging environments, while maintaining continuous functionality. The prevention of unexpected system shutdowns can be accomplished by the implementation of fault prognosis and isolation techniques inside the electric propulsion system. The analysis of the Permanent Magnet Synchronous Machine (PMSM) utilized in electric propulsion systems is examined in reference [13].

Electric vehicles (EVs) present issues related to the incidence of faults that are unavoidable during the continuous operation of the propulsion system. If these defects are not identified and rectified promptly, they can lead to safety risks, decreased operational effectiveness, and expensive malfunctions in the permanent magnet synchronous motor (PMSM) drives employed in electric vehicle (EV) systems [14]-[16]. Hence, it is important to conduct early fault detection of the electric vehicle (EV) propulsion system in order to avert severe failures and mitigate the expenses associated with maintenance procedures [14], [17]. The failures seen in permanent magnet synchronous motor (PMSM) drives may be categorized into three main types: electrical faults, mechanical faults, and magnetic faults [14], Figure 2.1 illustrates the steps of fault being detected in PMSM. The primary

motor failures are attributed to bearing defects and stator issues. Open circuit faults and short circuit faults are frequently observed in semiconductor switches and components. In contrast to faults observed in permanent magnet synchronous motor (PMSM) drives, semiconductor faults exhibit a tendency to induce breakdowns within a very brief timeframe. Battery-related defects can arise from fluctuations in battery voltages, currents, temperatures, and state of charge (SOC). Open circuit faults and short circuit faults employ three-phase current and three-phase voltage as indicators of problems. Open circuit fault diagnosis utilizes approaches that rely on voltage measurement and current measurement. The voltage measuring approach has the capability to identify the source of defects, but the current measurement method is ineffective in doing so [17].

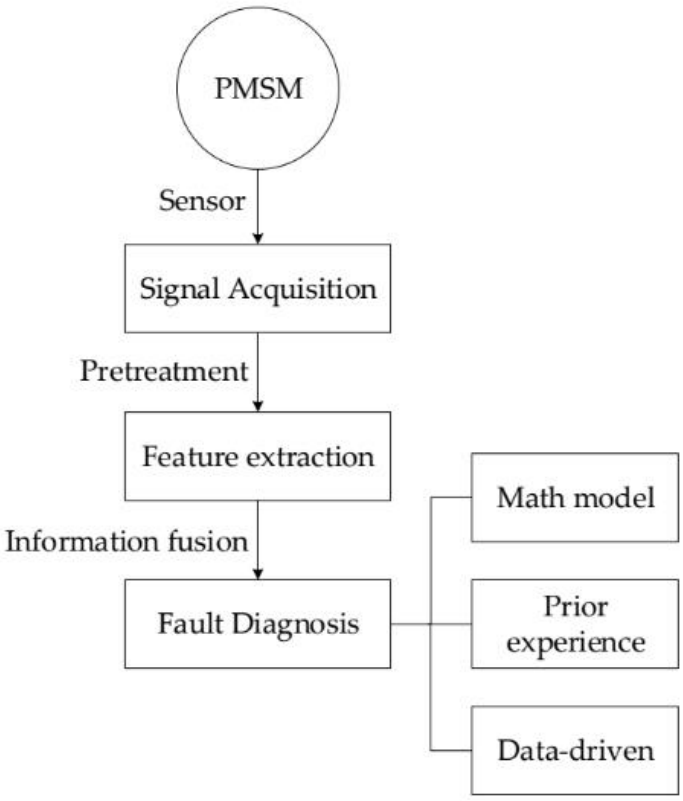

Figure 2.1: Fault Diagnosis Flowchart of Permanent Magnet Synchronous Motor (PMSM) [14]

In order to guarantee the safety, reliability, and availability of EV propulsion systems, it is imperative to incorporate Fault-Tolerant Control (FTC) mechanisms. The FTC (Fault-Tolerant Control) technique is predicated on the alteration of the topology of the Permanent Magnet Synchronous Motor (PMSM) drive system. This modification enables the system to maintain a constant operational speed even in the presence of faults or failures. In the study conducted by [15], a more advanced fault tolerant architecture for the electric vehicle (EV) drive system is presented. This particular topology employs a

decreased quantity of TRIAC switches and facilitates rapid detection of problems in both the lower and upper switches. The Federal Trade Commission (FTC) employs both passive and active approaches in its fault tolerance control system. In the passive method, the controller remains unchanged when a problem occurs, whereas in the active approach, the controller adjusts itself in response to the fault [19]. The uncertainties associated with faults are considered, and measures to control faults are incorporated during the design phase. The active approach relies on the collection of fault information, namely the identification of fault location and severity, through the utilization of a Fault Detection and Isolation (FDI) unit. In reference [18], a suggested technique is presented for sensorless fault-tolerant control (FTC) in electric vehicles (EVs) utilizing induction motor drives (IMDs). This strategy incorporates the use of Backstepping Control (BC) with the Extended Kalman Filter (EKF) algorithm. In order to identify instances of faults, several studies have yielded findings by employing real-time simulation techniques, such as Digital Twin (DT) and Hardware-in-the-Loop (HIL), for electric vehicle (EV) propulsion drive systems. Digital Twin (DT) is a methodology that involves the creation of a simulated environment by utilizing real-world data and including inputs and outputs from the controlled system. This enables the replication of the system's operations within the virtual realm. Hence, the utilization of Decision Trees (DT) may be employed for the purpose of monitoring the health of Electric Vehicle (EV) propulsion systems, diagnosing faults, optimizing performance, and assessing potential risks. High-level simulation (HIL simulation) is a methodology that involves substituting the physical system with a test system consisting

of both hardware and software components. This test system is designed to interact with genuine input and output signals from a controller. Nevertheless, DT exhibits a higher level of superiority compared to HIL in terms of its capability to conduct comprehensive testing on a complete model of a physical drive system [16]. Moreover, the field of literature [16] offers valuable insights into various methodologies employed in the context of DT and HIL in electric vehicle propulsion systems. Additionally, it is proposed to utilize a mix of DT (Discrete-Time) and HIL (Hardware-in-the-Loop) models in order to demonstrate the viability of the controller. These DT models are constructed based on HIL simulation experiments that have been conducted in prior research [4]-[6], and as demonstrated in Figure 2.2.

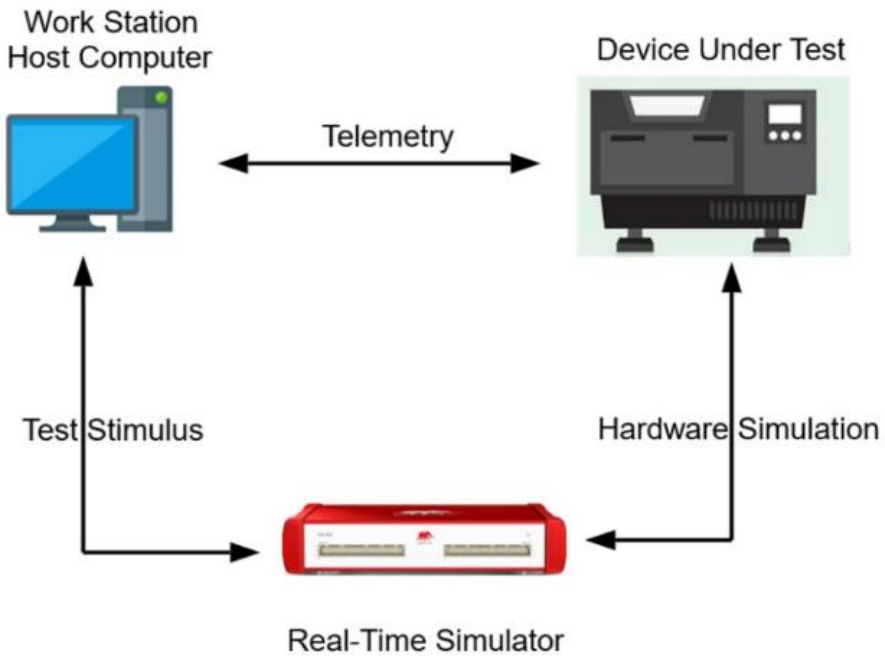

Figure 2.2: Hardware-in-the-Loop System (HIL System) [16]

2.2 Signal Processing Techniques

Signal processing techniques can be used to detect faults in a electrical system. Literature of different techniques have been found. Power systems are of utmost significance in contemporary society, as they fulfill a crucial function. It is imperative to prioritize the maintenance of their dependability and stability.

Changes in signals can be detected by many signal processing methods. In the past decades, a range of strategies have been used to identify and separate defects in electric vehicle propulsion drive systems. These strategies may be categorized into three main groups: model-based fault diagnosis techniques, signal-based fault diagnostic methods, and data-driven approaches [14]. The Finite Element Model (FEM) has higher precision and computational cost relative to alternative models. One of the benefits of the Finite Element Method (FEM) is its ability to incorporate physical and geometric aspects into the modeling of mechanical flaws using finite element field computation [14]. Signal-based fault procedures encompass many methods such as Motor Current Signal Analysis, Fast-Fourier Transform (FFT), Short-Time Fourier Transform (STFT), and Wavelet Transform (WT) in [14], [21] and [22]. Nevertheless, it should be noted that these methodologies exhibit a certain degree of sensitivity towards temporary disturbances and do not yield optimal precision when both the temporal and frequency domains of the signal are jointly evaluated. Artificial Neural Networks (ANN) and Deep Learning (DL) are extensively employed in data-driven fault diagnostic techniques for the purpose of defect identification and severity assessment. Artificial Neural Networks (ANNs) have been found to yield

enhanced accuracy in many tasks. However, the utilization of a substantial dataset for training purposes presents a computational load, necessitating the allocation of extra hardware resources. An Artificial Intelligence algorithm has been employed for the purpose of identifying defects in the voltage source inverter (VSI) inside the propulsion system. The utilization of this technology resulted in the elimination of superfluous hardware and demonstrated the effective integration of its software logic into an on-board health monitoring system. Furthermore, the utilization of data-driven techniques has proven to be effective in the detection of internal imbalances resulting from electrical and mechanical problems in the Permanent Magnet Synchronous Motor (PMSM) [19]. Nevertheless, it is important to acknowledge that data-driven approaches do possess certain drawbacks, particularly in terms of the intricate nature of higher classification and feature extraction processes. Deep learning models, such as Convolutional Neural Networks (CNNs), which are formed from a Feed Forward Network (FFN), provide an innate capability to categorize raw data without the need for further feature extraction processes. This characteristic has been seen to result in improved accuracy [14].

The authors of the cited literature [17] introduced a one-dimensional convolutional neural network (CNN) model for the purpose of diagnosing three distinct states of operation in permanent magnet synchronous motors (PMSMs). This model was designed to effectively handle a broad spectrum of motor speeds, fluctuating loads, and eccentricity effects. The fault diagnostic approach successfully categorized the motor states into three distinct categories: fault-free state, demagnetization fault state, and bearing fault state.

Regarding the superiority of the 1D CNN model, it exhibited a final accuracy rate of 98.85%, surpassing that of traditional machine learning techniques such as KNN (K-nearest Neighbor) and SVM (Support Vector Machine). In contrast to the previous study, the utilization of a one-dimensional convolutional neural network (1D CNN) yielded superior outcomes in terms of accuracy rates pertaining to the motor failure mechanism. A different study [20] categorizes defect diagnostic approaches into two groups: model-free methods and model-based methods. The model-based approach utilizes the pre-existing characteristics of the dynamic model of the electric drive system in its normal operating condition.

The model-based approach is considered to be more advantageous compared to the model-free approach due to its ability to effectively identify and isolate many defects inside the system [19]. In the study conducted by [19], the researchers utilized a model-based technique to detect and isolate incipient faults. Following the acquisition of health indicators derived from an onboard sensor, a hierarchical prognostic algorithm was employed to identify and isolate the early-stage defects. The algorithm employed a rule-based methodology, initially conducting a performance diagnosis of the drive system. This involved assessing the system-level health indicators of the drive system. Subsequently, the algorithm proceeded to compare the component-level health indicators in order to identify the specific component responsible for the degradation, commonly referred to as the faulty component. In a recent study by the authors [20], a novel model-free approach was proposed for training a neural network utilizing input-output data acquired from the

faultless operation of the Permanent Magnet Synchronous Motor (PMSM). The fault detection and isolation (FDI) approach, as described in the literature [20], has been successfully applied to various dynamic systems, including motors and power electronics converters used in electric traction systems. Figure 2.3 shows a design of the mentioned EV traction system. This approach utilizes neural networks with Gauss-Hermite activation functions to model the permanent magnet synchronous motor (PMSM) and effectively detects incipient failures. The defects were separated in this manner by utilizing the statistical features of the observed signals, which revealed the particular component of the Permanent Magnet Synchronous Motor (PMSM) that was experiencing failure.

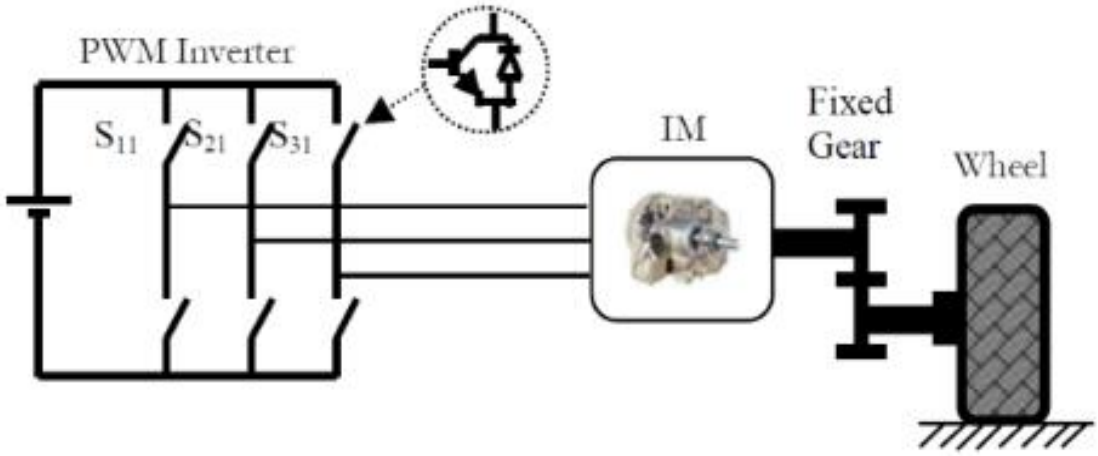

Figure 2.3 EV Traction System Scheme [18]

2.3 Three-Phase Inverter Design

The utilization of three-phase inverters holds significant importance in many industries, as they possess the capability to transform direct current (DC) power into alternating current (AC) power, hence generating three-phase outputs. The main types of three-phase inverter are Voltage Source Inverter (VSI), Current Source Inverter (CSI), Multilevel Inverter, Resonant Inverter, etc. These are some of the most common varieties of three-phase inverters, each of which is suited to specific applications based on voltage and current requirements, efficiency, and waveform quality. The type of inverter selected depends on the application's specific requirements and the intended performance characteristics.

The inverter can be treated as a converter, but functions in a DC-AC mode [23], [24]. The most common topology of three-phase VSI is shown in Figure 2.4. This topology has three legs, each leg provides a single-phase voltage to the load. There is a diode paired with each switch.

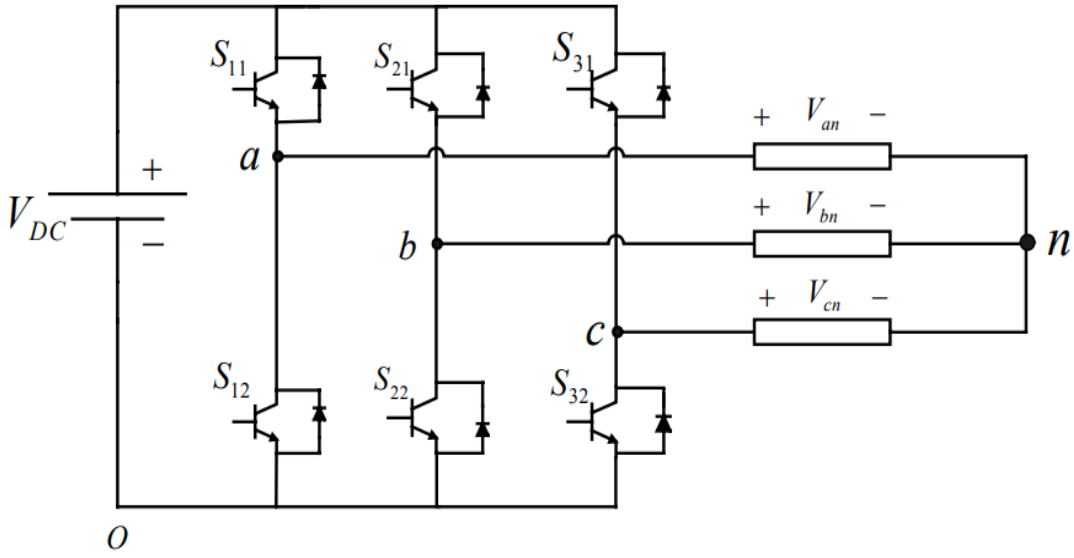

Figure 2.4: Three-phase Inverter topology [45]

The inverter is powered by a DC supply. The semiconductor switches operate in either the saturated or cut-off regions of the i-v characteristics. Theoretically, this will eliminate power losses (since neither voltage nor current will be present) [25], [26].

We need to apply control strategy for the inverter to obtain our design goal. There are several common strategies, the most classic type is Pulse Width Modulation (PWM). This classic method aims to generate a sinusoidal output voltage by varying the width of the inverter's switching pulses based on the reference sinusoidal waveform. It is widely used in applications where low distortion and high-quality output voltage are required [27]-[30]. Field-Oriented Control (FOC) is predominantly utilized in motor drive applications. It controls the orientation and current of the motor's magnetic field independently, allowing for precise control of torque and speed. It is utilized frequently in high-performance motor

drivers [31]-[35]. Another reliable technique is the Proportional-Integral Control (PI Control). The application of PI control is frequently observed in conjunction with other control methodologies for the purpose of regulating diverse parameters, including but not limited to DC bus voltage, output voltage, or current. The technique offers consistent and reliable accuracy in maintaining a steady-state condition, and is frequently utilized in voltage and current control systems [36]-[42].

Chapter 3. Methodology and Engineering Design

In this chapter, we will go through the methodology and designs in various systems and in different perspectives of fault detection concept. We will firstly present a design that is able to diagnose, monitor, and broadcast faults in the system. Secondly, we will go in details into the conventional 3-phase inverter model. Lastly, the selected elements will be discussed.

3.1 Signal Processing Methodology

To design a sensorless system to diagnose, monitor, ad broadcast faults, a signal processing mixed clustering technique was applied. The clustering technique uses a data-mining approach to detect failures for predictive maintenance planning.

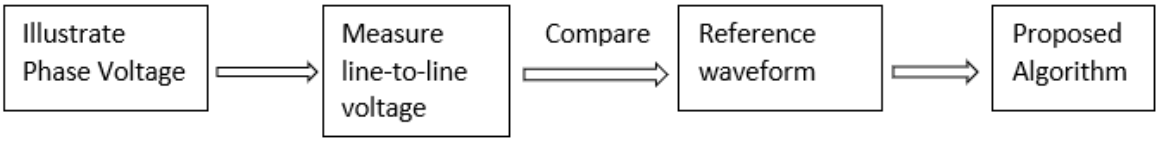

Figure 3.1 Open Circuit Switch in VSI (fault case)

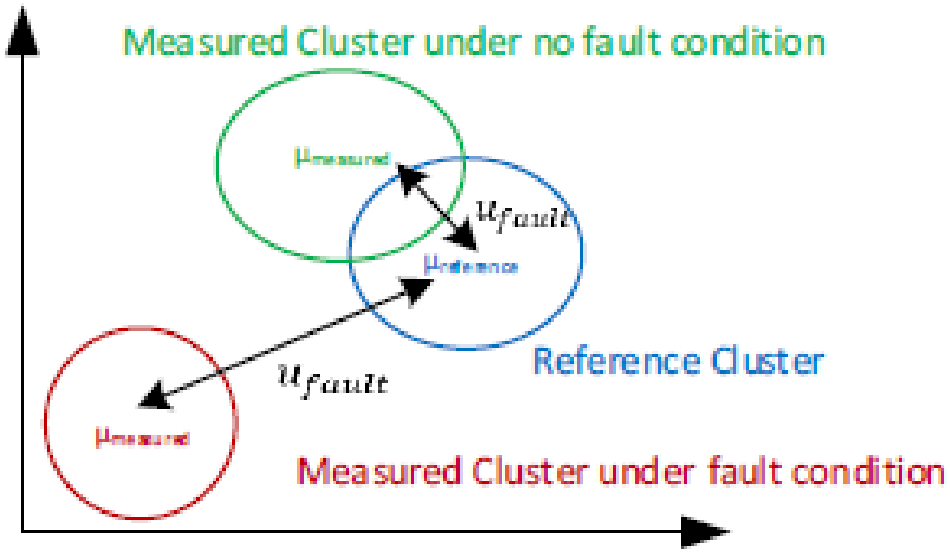

Figure 3.2 Block Diagram of The Clustering Method

Clustering approach can be used to detect faults in the Voltage Source Inverter (VSI), as shown in Figure 3.1. The first step is to find out the phase voltage, then the line-to-line measurement will be implemented. To detect faults in the phase voltage, a reference cluster is formed by the captured reference waveform generated by the gated driver. The generated phase voltage waveform, matching the previously captured reference waveform, is recorded and categorized as the measured cluster within the same time frame. Next step is to access the intersection of the reference frame and the measurement. After all the steps are completed, a conclusion of the fault occurrence will be determined, which is based on computing the mean of the measured and reference clusters. The population mean is calculated by Equation (3.1).

$$\mu = \frac{1}{N}\Sigma_{i=1}^{N} x_i \tag{3.1}$$

N is the total number of the sample signals, μ is the mean, and x_i is the desired cluster's sample data. Equation (3.2) shows the method to find out the standard deviation of the reference and to make the decision of the occurrence of fault.

$$\sigma = \sqrt{\frac{1}{N}\Sigma_{i=0}^{N}(x_i - \mu)^2} \tag{3.2}$$

N is the total number of sample signals, σ is the standard deviation, x_i is the cluster's sample data and μ standards for the average of the reference cluster.

The mean of the produced waveform can be calculated by Equation (3.3). The purpose is to identify whether it is in the range of the reference cluster or not.

$$\mu_{fault} = \begin{cases} 0, & \mu_{ref} - \frac{1}{2}\cdot\sigma_{ref} < \mu_{measured} < \mu_{ref} + \frac{1}{2}\cdot\sigma_{ref} \\ 1, & Otherwise \end{cases} \tag{3.3}$$

Where $\mu_f$is the existence of fault, $\mu_{measured}$ stands for the mean of the tested cluster, μ_{ref} is the average value, and σ_{ref} is the reference cluster's standard deviation. When the measured signal's mean value locates in the range of the half of the value of reference's average standard deviation, that means no fault was found. When the mean value of the captured signal is beyond the range, it indicates a fault has occurred.

The decision process was inspired by the Gaussian distribution, as shown in Figure 3.3. the collected cluster should be close to the reference with no more than ±19.5% deviation, in order to avoid labelling the generated signal as a fault. Considering the parasitic of the semiconductor, the real model, and the transient, we expanded the comparison range to include half standard deviation.

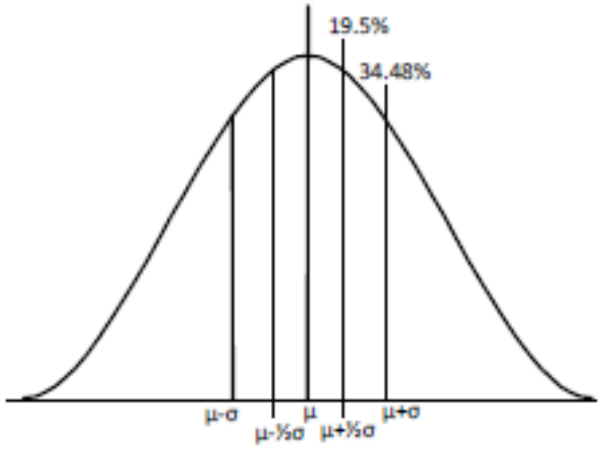

Figure 3.3 Gaussian distribution

3.2 Modeling of SPWM

In this thesis, PWM and SPWM methods are implemented to generate the pulse width modulation. PWM and SPWM modeling methods differ primarily in their ability to replicate waveform shape and harmonic contents. PWM provides a square wave approximation and has more harmonic contents, while SPWM closely follows the shape of

the reference waveform, resulting in reduced harmonic distortion. We can obtain a controlled output voltage from the ac side according to adjusting the pulse width of the inverter components based on the on and off periods, while the dc voltage stays as a fixed value [43]. Equation (3.4) is used to calculate the duty cycle.

$$D = 0.5 + (A \,/\, 2) \cdot sin(2\pi \cdot f_{Carrier} \cdot t) \tag{3.4}$$

The SPWM method considers each modulating voltage individually and then compare to the carrier triangular waveform [44]. The modulation index of the amplitude and frequency are defined by Equation (3.5) and Equation (3.6), respectively.

$$m_a = \frac{Peak\ of\ V_{ao1}}{V_{d/_2}} = \frac{V_{control}}{V_{triangle}} \tag{3.5}$$

$$m_f = \frac{f_s}{f_o} \tag{3.6}$$

V_{ao1} is the fundamental component of V_{ao}. $V_{control}$ is the peak value of the control signal. $V_{triangle}$is the peak value of the triangular waveform. The voltage values involved in this calculation should be the line to line and line. m_a is the modulation index and should be no more than 1, to perform within the linear region of modulation and avoid overmodulation results [45]. f_s is the output frequency that we are aiming for, which is determined by the frequency of the reference.

3.3 Modelling of RCD Snubber

In this thesis, we aimed to design a system which takes low voltage as input and obtain a much higher voltage as an output. In this process, we need to come up with a system to protect the circuit when the voltage is beyond the limits. RCD snubber are commonly used in various applications, for example motor drives, power converters, and switching power supplies. In this thesis, we used the RCD snubber circuit to protect electronic components, from the harmful effects of the voltage spikes that could possibly cause overvoltage breakdown. The schematic of the RCD circuit is shown in Figure 3.4. When Q1 is turned off, and when duty cycle is smaller or equal to 0.5, the capacitor C has the maximum capacity and the ripple voltages at both ends are the maximum. Equation (3.7) and (3.8) are used to calculate the C_m and ΔV_{Cm}, respectively.

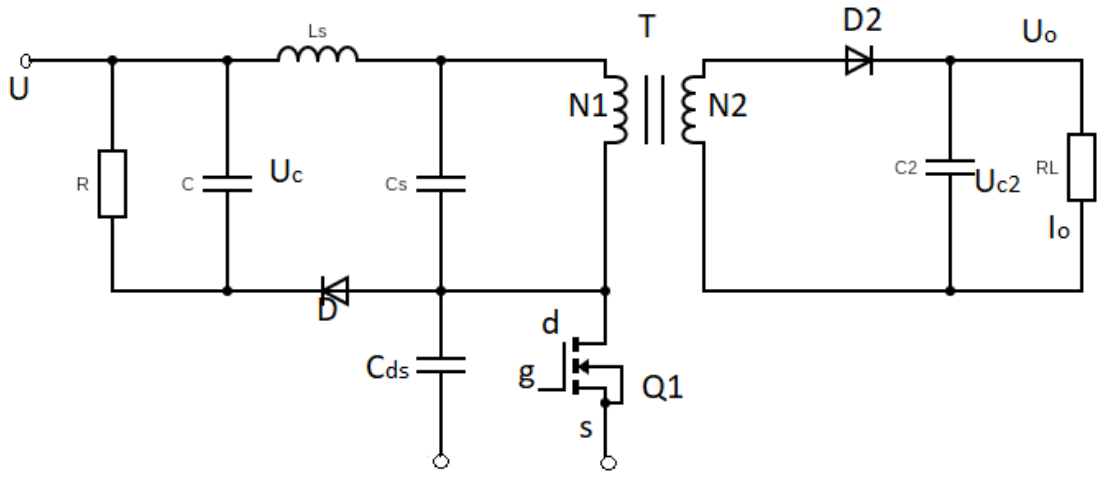

Figure 3.4 RCD Circuit Schematic, adapted from [46]

$$C_m = L_s\left(\frac{I_m}{\Delta V_c}\right)^2 = rL_s\left(\frac{V\cdot T_{on}}{L\cdot\Delta V_c}\right)^2 \tag{3.7}$$

$$\Delta V_{cm} = I_m\sqrt{\frac{Ls}{C_m}} = \frac{V\times T_{on}}{L_\mu + L_s}\sqrt{\frac{L_s}{C_m}} = \frac{V\times T_{on}}{L}\sqrt{\frac{L_s}{C_m}} \tag{3.8}$$

In Equation (3.7) and (3.8), V is the input voltage, ΔV_c is the change of the ripple voltage. I_m is the maximum value of the excitation current flowing through the primary coil of the transformer. L_s is the inductance of the primary side of the transformer, L_u is the exciting inductance of the transformer's primary side, so that L will be total inductance for the primary side. T_{on} is the period of time when the switch Q_1 is turned on.

In real life, we need to consider the effects of resistance of R, which can influent the amount of current flowing through the capacitor. In addition, the leakage current will decrease, when the switch Q1 is turned off from the ON mode, this will also affect the amount of current flowing through the capacitor [47], Equation (3.7) and (3.8) can be rewritten as (3.9) and (3.10) , respectively.

$$C = L_s\left(\frac{rI_m}{\Delta V_c}\right)^2 = rL_s\left(\frac{rV\cdot T_{on}}{L\cdot\Delta V_c}\right)^2 \tag{3.9}$$

$$\Delta V_c = rI_m\sqrt{\frac{Ls}{c}} = r\frac{V\times T_{on}}{L_\mu + L_s}\sqrt{\frac{L_s}{C}} = r\frac{V\times T_{on}}{L}\sqrt{\frac{L_s}{C}} \tag{3.10}$$

Here, r is a coefficient related to the resistance R and the capacitance between the D-S pole of the switch C_{ds}, its value is $0 \le r \le 1$. When r = 1, the resistor R is open, and

Cds is 0, so that the capacitance of C and ripple voltage ΔV_c in Equation (3.9) and (3.10) will be the same as Equation (3.7) and (3.8).

Equation (3.11) to (3.13) are used to calculate the resistance, capacitance, and ripple voltage.

$$\left(V_{paL} + \frac{1}{2}\Delta V_c\right) e^{-\frac{T_{ON}}{RC}} = V_{paL} - \frac{1}{2}\Delta V_c \tag{3.11}$$

Or Equation (3.11) can be rewritten as (3.12).

$$e^{-\frac{T_{ON}}{RC}} = \frac{V_{paL} - \frac{1}{2}\Delta V_c}{\left(V_{paL} + \frac{1}{2}\Delta V_c\right)} \tag{3.12}$$

$$\frac{T_{ON}}{RC} = -\ln \frac{(V_{paL} - \frac{1}{2}\Delta V_c)}{(V_{paL} + \frac{1}{2}\Delta V_c)} \tag{3.13}$$

Where, V_{paL} is the half-wave average of the transformer primary side flyback output voltage. Before we apply Equation (3.11) to (3.13), we need to find out the capacitance and ΔV_c by using Equation (3.7) to (3.10). In the RCD circuit, the charging capacity is determined by capacitor C, and discharging capacity is determined by the resistor, and they have to be in a balanced mode to achieve the best performance of the circuit [46].

3.4 PWM Controller

In order to protect the RCD circuit and make sure its performance in a good condition, we need to find a component to monitor and control the power flow in the circuit. Pulse Width Modulation (PWM) is quite a common way for the control method. The electrical energy will be increased or decreased by adjusting the pulse width of the input signal, which can lead to the change of output voltage or output power supply. To be more specific, when the input pulse width is increased, the output voltage will be increased, and when the pulse width is reduced, the output voltage will be reduced. This modulation provides a closed-loop feedback control for the output voltage [47], [48].

The UC384x family are fixed frequency PWM controllers. They are specially designed for off-line and DC-to-DC converter applications and require minimal external components. The internally implemented circuit consist of a trimmed oscillator for the precise duty cycle control, a reference for temperature compensation, a high gain error amplifier, a current-sensing comparator, and also a high-current totem pole output, which is ideally designed for driving a power MOSFET [50]. The selected controller in this thesis is UC3434, based on the threshold voltage in the design, the startup voltage is 12 V and better adjustments with the duty cycle of the switch. The Table 3.1 introduces the differences among the UC384x family.

Table 3.1 Differences of UC384x

Size	Threshold Voltage (ON)	Threshold Voltage (Off)	Duty Cycle	Frequency
UC3842	16 V	10V	0 – 100%	Up to 500KHZ
UC3843	8.5 V	7.9V	0 – 100%	Up to 500KHZ
UC3844	16V	10V	0 – 50%	Up to 500KHZ
UC3845	8.5V	7.9V	0 – 50%	Up to 500KHZ

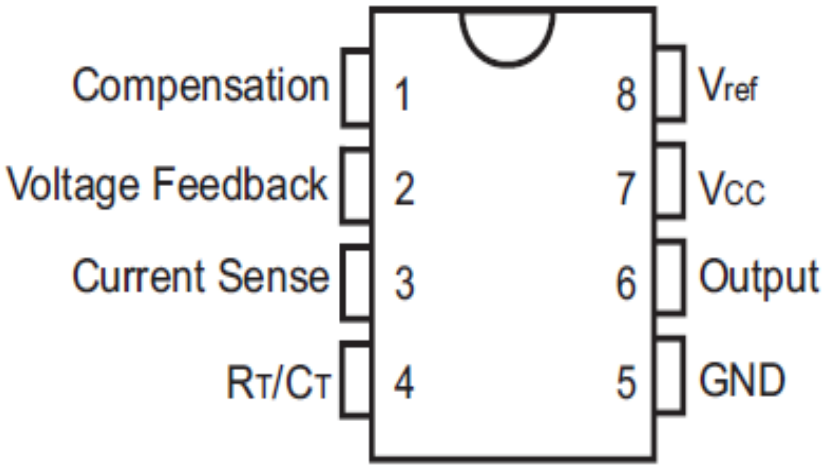

Figure 3.5 Pin Configuration of UC3843 – Top View [50]

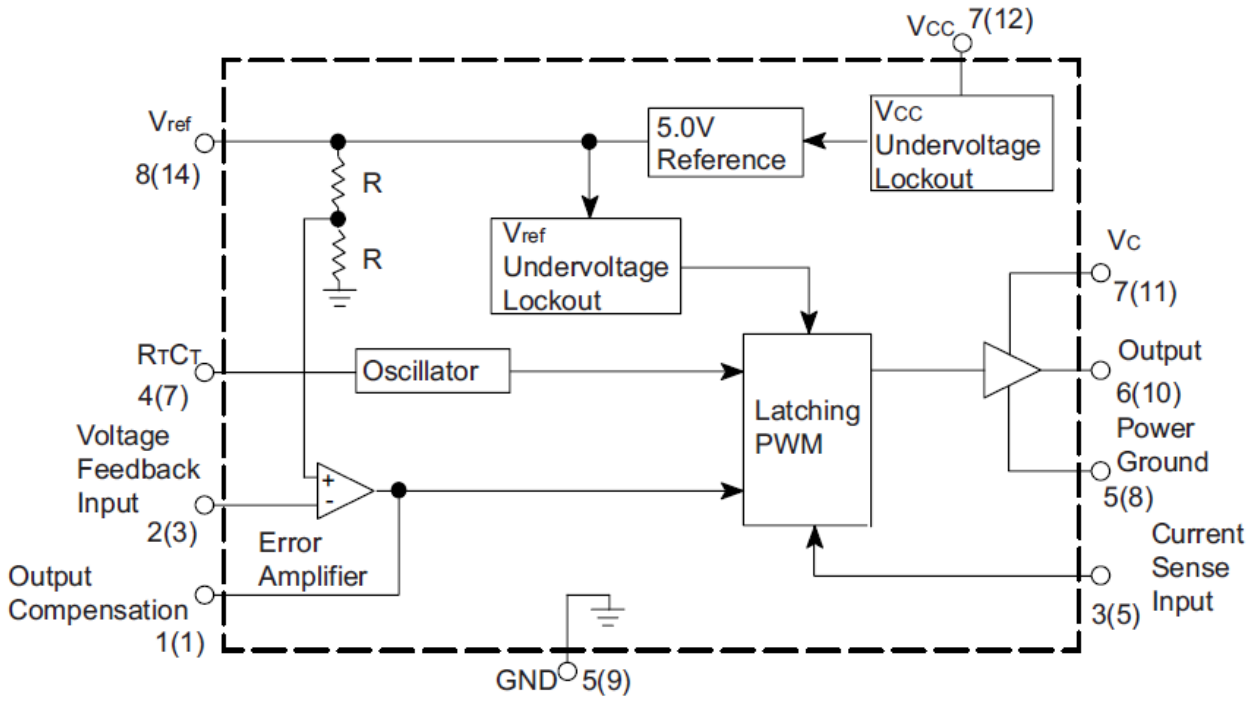

Figure 3.6 Simplified Block Diagram [3.8]

The selected controller has 8 pins, as shown in Figure 3.5. Pin 1 is the compensation; it is the Error Amplifier output. Pin 2 is the voltage feedback. Pin 3 is the current sense. Pin 4 indicates R_T/C_T, which reflects the Oscillator frequency. Pin 5 is to be grounded. Pin 6 connects to the output. Pin 7 is the V_{CC} side, and Pin 8 is the reference output V_{REF}. Figure 3.6 is the simplified block diagram for the internally implemented circuit of UC3843 PWM controller. To get the desired oscillator frequency with certain values of resistor and capacitor, this thesis follows the performance characteristics as shown in Figure 3.7. In this figure, we can see the relationship among the timing resistor, timing capacitor and the corresponding oscillator frequency. When the R_T is 7.5 KΩ and

C_T is 2.2 nF, the frequency can be found as approximately 100 KHz. The relationship between the output deadtime and oscillator frequency can be found in Figure 3.8.

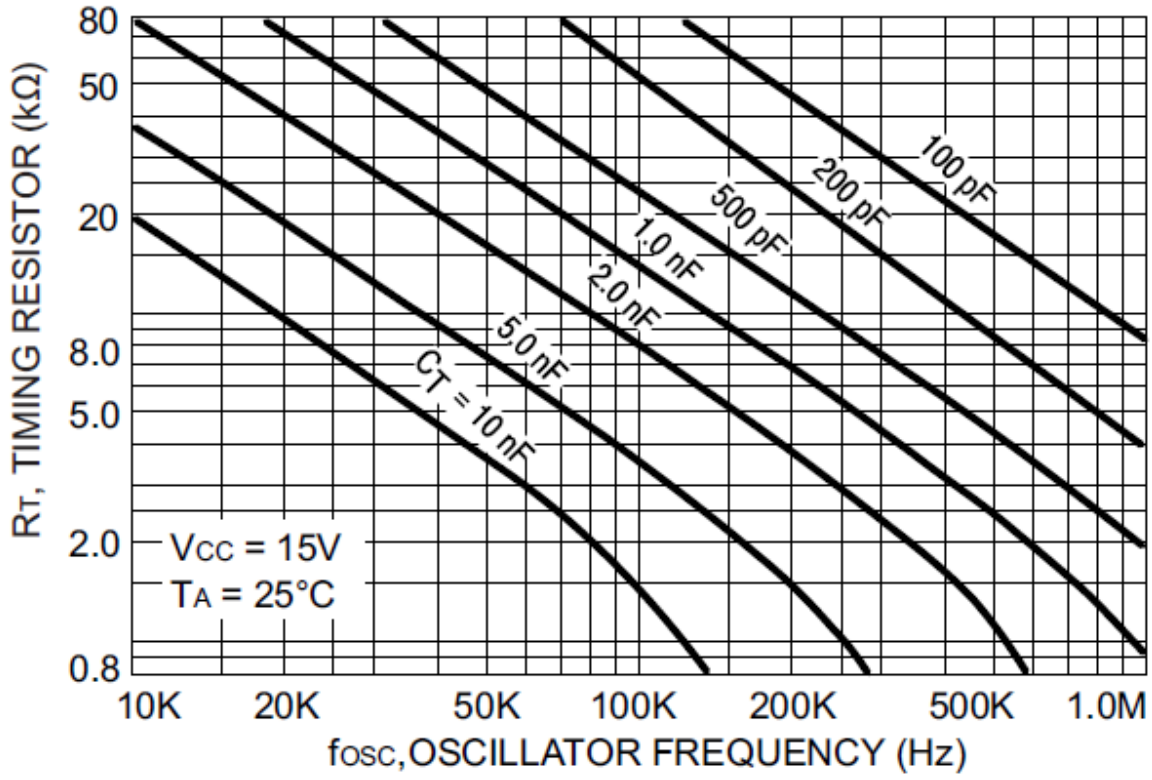

Figure 3.7 Timing Resistor and Oscillator Frequency [3.8]

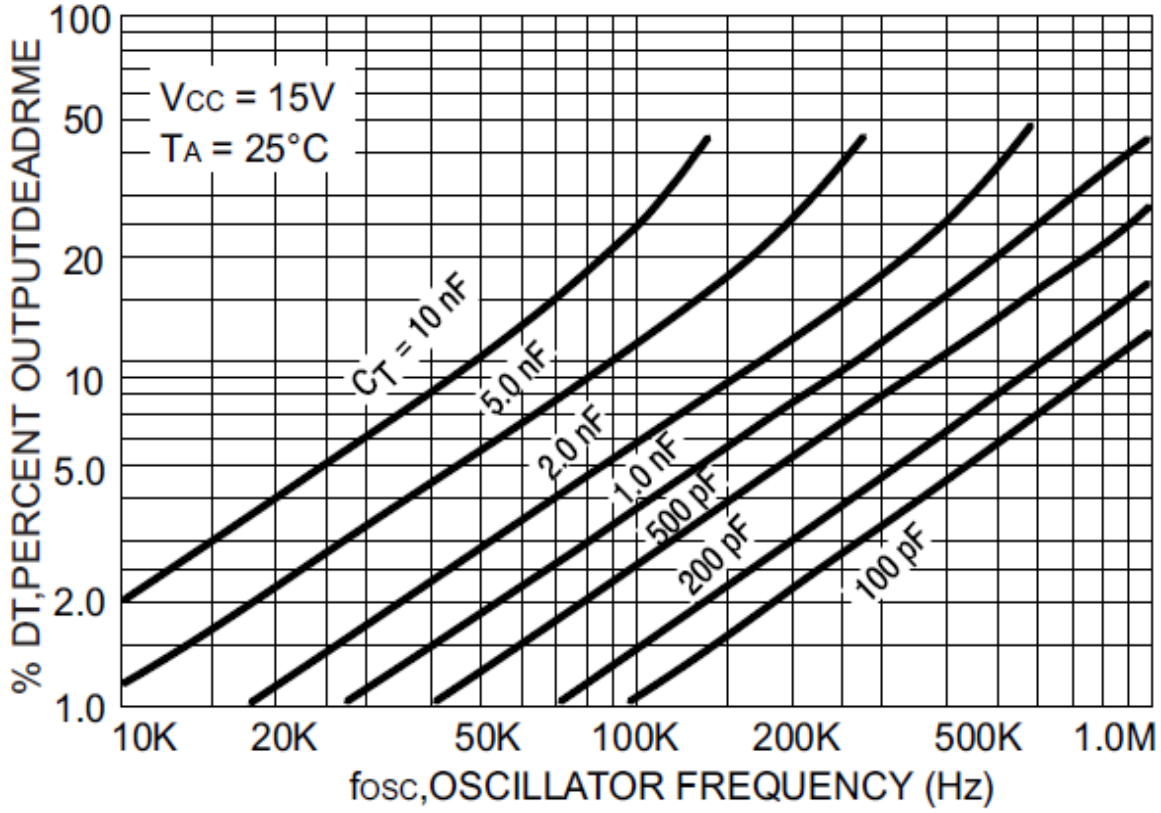

Figure 3.8 Output Deadtime and Oscillator Frequency [3.8]

In addition to utilize the performance characteristics in Figure 3.7, the Oscillator frequency in Pin 4 can be calculated by Equation (3.14).

$$f = \frac{1.72}{R_T \times c_T} \tag{3.14}$$

When R_T is 7.5 KΩ and C_T is 2.2 nF, f can be calculated as 105.7 KHz.

3.5 Design of the Optocoupler Circuit

In this thesis, the input is a low DC voltage and the output is a much higher DC value. To protect the circuit and electrical components, an isolation system is required. Optocouplers based Si IGBTs are the most commonly operated ones. These gate drivers, especially the simpler ones, provide the high peak current required to enable the IGBT gate terminal's quick switch position. Additionally, they provide electrical isolation between the power side of the gate driver and the signal side (such as the control circuity) [51], [52]. The more complicated design of the gate driver can protect the Safe Operating Area (SOA) of the IGBT and prevent it from over flow of voltage, current or over heat of the device [53].

Our goal is to transmit the signal to the secondary side from the primary side, we implement an optocoupler circuit design. The circuit should be similar as Figure 3.9.

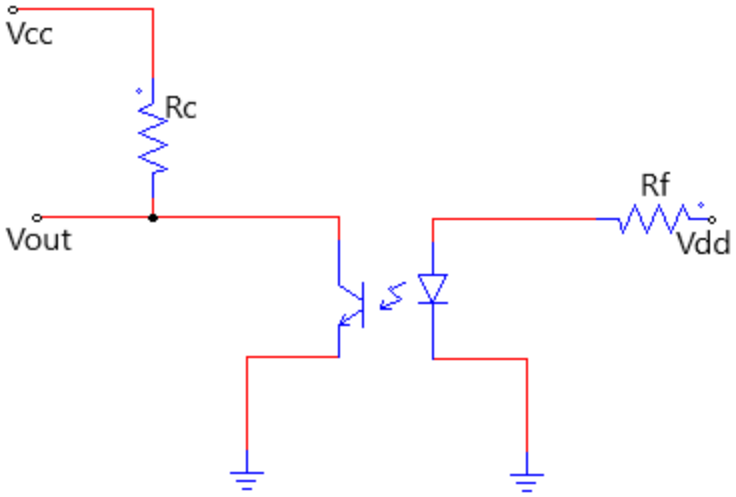

Figure 3.9: Optocoupler Circuit

The circuit shown above could be arranged to work at linear or saturation regions. V_{out} node should be ideally zero for the saturation case; in linear region, the V_{out} shou be larger than zero but lower than V_{cc}. Optocoupler has a current transfer ratio (CTR), which is similar to the idea of BJT's current gain. Equation (3.14) can be used to calculate the CTR of the optocoupler. Equation (3.15) and (3.16) can be used to find the parameters for the corresponding components [53].

$$CTR = (I_c/I_f) * 100\% \tag{3.14}$$

$$I_f = \frac{(V_{dd}-V_f)}{R_f} \tag{3.15}$$

So that Rf can be found by Equation (3.15), where V_f is the forward voltage of the optocoupler.

$$R_f = I_f\left(V_{dd} - V_f\right) \tag{3.16}$$

As we know, there are two settings for the optocoupler circuit, one is the saturation mode and the other one is linear mode. When the ration of I_c/I_f is smaller than CRT, than the optocoupler is in the saturation setting, $I_{c,sat}$ and R_c can be determined by Equation (3.17) and (3.18). However, when the I_c/I_f is equivalent to the CRT, it is in the linear setting, I_c and R_c can be determined by Equation (3.19) and (3.20), respectively.

$$I_{c,sat} = \left(V_{cc} - V_{CE,sat}\right) / R_c \tag{3.17}$$

$$R_c > \frac{V_{cc} - V_{CE,sat}}{CTR \times I_f} \tag{3.18}$$

$$I_c = \left(V_{cc} - V_{CE}\right) / R_c \tag{3.19}$$

$$R_c = \frac{V_{cc} - V_{CE}}{CTR \times I_f} \tag{3.20}$$

3.6 Modeling of Three-Phase Voltage Inverter

According to Fourier Analysis, the line-to-line voltage v_{ab}, v_{bc}, and v_{ca} can be determined by Equation (3.21) to (3.23).

$$V_{ab}(t) = \sum_{n=1,3,5,\ldots}^{\infty} \frac{4V_{dc}}{n\pi} cos\frac{n\pi}{6} sin\, n\left(\omega t + \frac{\pi}{6}\right) \tag{3.21}$$

$$V_{bc}(t) = \sum_{n=1,3,5,\ldots}^{\infty} \frac{4V_{dc}}{n\pi} cos\frac{n\pi}{6} sin\, n\left(\omega t - \frac{\pi}{2}\right) \tag{3.22}$$

$$V_{ca}(t) = \sum_{n=1,3,5,\ldots}^{\infty} \frac{4V_{dc}}{n\pi} cos\frac{n\pi}{6} sin\, n\left(\omega t - \frac{7\pi}{6}\right) \quad (3.23)$$

The Three-phase inverter circuit diagram is illustrated as in Figure 3.10. The line-to-ground can be computed by Table 3.2.

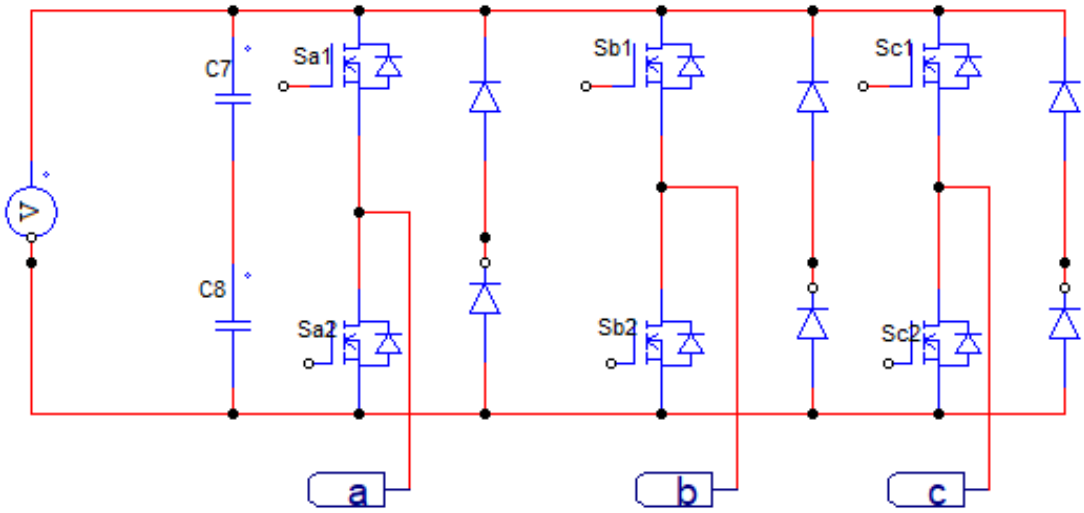

Figure 3.10 Three-Phase Inverter Circuit Diagram [54] – (Reproduced in PSIM)

Table 3.2 Three Phase Inverter – Voltage Calculations

Mode	$V_{line\text{-}to\text{-}line}$		
$0 \leq \omega t \leq 60°$	$v_{ab} = V_{dc}$	$v_{bc} = -V_{dc}$	$v_{ca} = 0$
$60° \leq \omega t \leq 120°$	$v_{ab} = V_{dc}$	$v_{bc} = 0$	$v_{ca} = -V_{dc}$
$120° \leq \omega t \leq 180°$	$v_{ab} = 0$	$v_{bc} = V_{dc}$	$v_{ca} = -V_{dc}$

The rms value of the line-to-line voltage can be determined by Equation (3.24). In addition, Equation (3.25) can be used to find the line-to-neutral voltage rms value.

$$V_L = \left[\frac{1}{\pi}\int_0^{\frac{2\pi}{3}} v_s^2 \, d(\omega t)\right]^{\frac{1}{2}} = 0.8165 V_S \tag{3.24}$$

$$V_p = \frac{V_L}{\sqrt{3}} = \frac{\sqrt{2}\, V_S}{3} = 0.4714 V_S \tag{3.25}$$

Chapter 4. Simulation Results of Design

To simulate the design, PSIM software and MATLAB Simulink were used. The PSIM design was inspired by a templated offered by PSIM for inverter designs, it was used as a starting point and modified for the desired functions and features.

4.1 Simulation Results of Clustering Method

With the help of MATLAB Simulink, as well as the Simscape Library IGBT model, the simulation was implemented successfully. Based on the specifications of EV ratings, and AC inverter as the main application, the selected IGBT was from SEMIKRON, SEMiX453GB12E4. Table 4.1 provides the important characteristics and system specifications of this component.

Table 4.1. Specifications of the SEMIKRON IGBT

Parameter	Value	Unit
Voltage Rating	1200	V
Current Rating	683	A
Parasitic Capacitance (C_{ies}, C_{oes}, C_{res})	27.9; 1.74; 1.53	nF
DC bus Link	300	V
Load (Equivalent model of Chey Volt electric motor)	5 Ω + 30 mH	

Table 4.2 includes the results of the simulation whether there is an open circuit fault or not. The parameters, healthy cases, faulty cases and diagnosis are listed.

Table 4.2. Results from simulation and experiments of different cases

Parameter	Simulation Healthy	Simulation Faulty	Practical Healthy	Practical Faulty
Reference Average	0.5108	0.5108	0.3957	0.4381
Reference Standard Deviation	0.4999	0.4999	0.4759	0.5084
Measured Cluster Average	0.5097	0.0086	0.4499	0.7012
Diagnosis	No Fault Occurred	Fault Occurred	No Fault Occurred	Fault Occurred

When there is no fault detected in the circuit, by comparing the gate driver reference signal to the normalized phase voltage when the fault had not occurred, it is possible to determine the conclusion that the waveforms overlap, as shown in Figure 4.1. The

discrepancy will be caused by the IGBT model's reality behavior. In Figure 4.2 and 4.3, it is clear to see that the fault was detected.

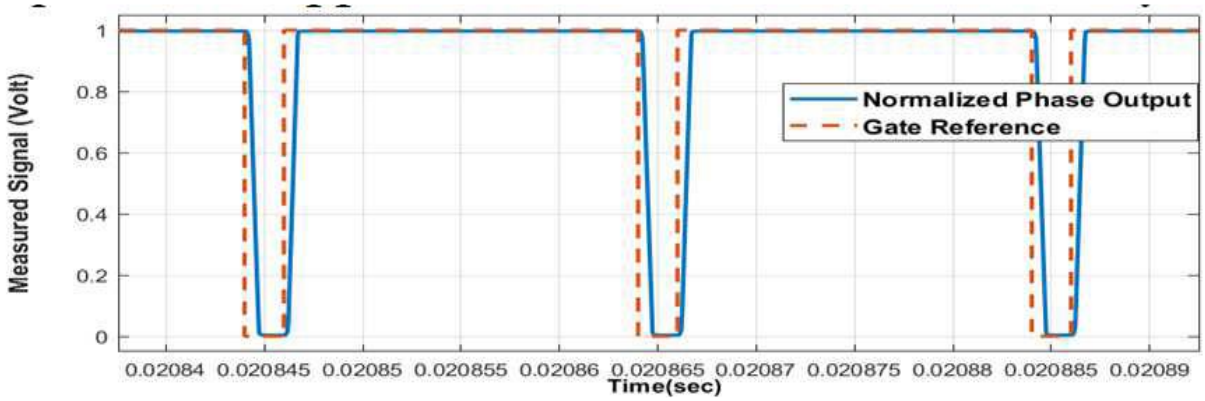

Figure 4.1 The Generated and Reference Waveform – No Fault

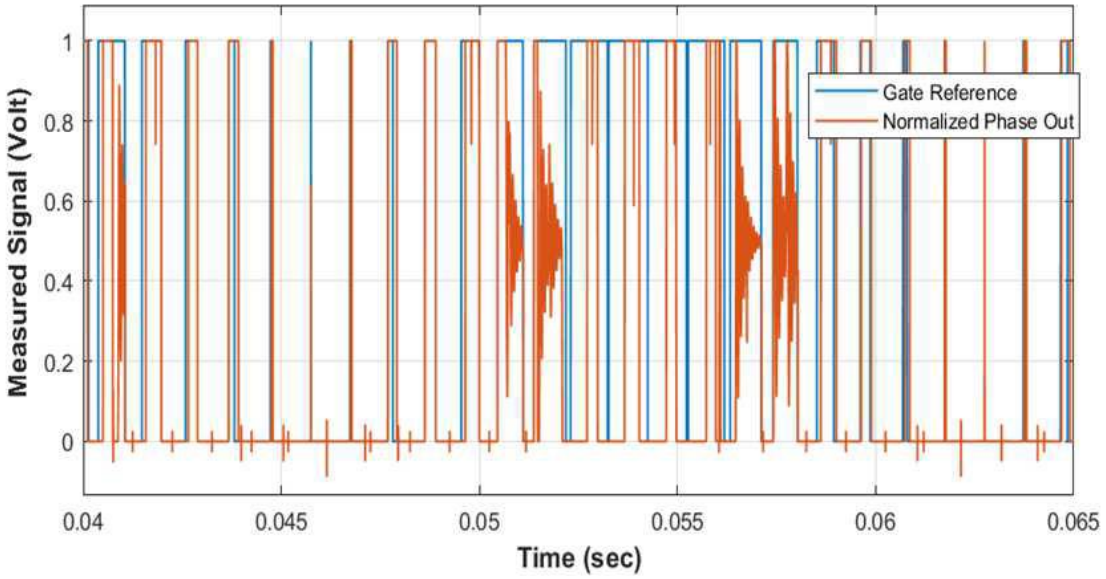

Figure 4.2 The Output and Reference Waveform – Fault Occurred

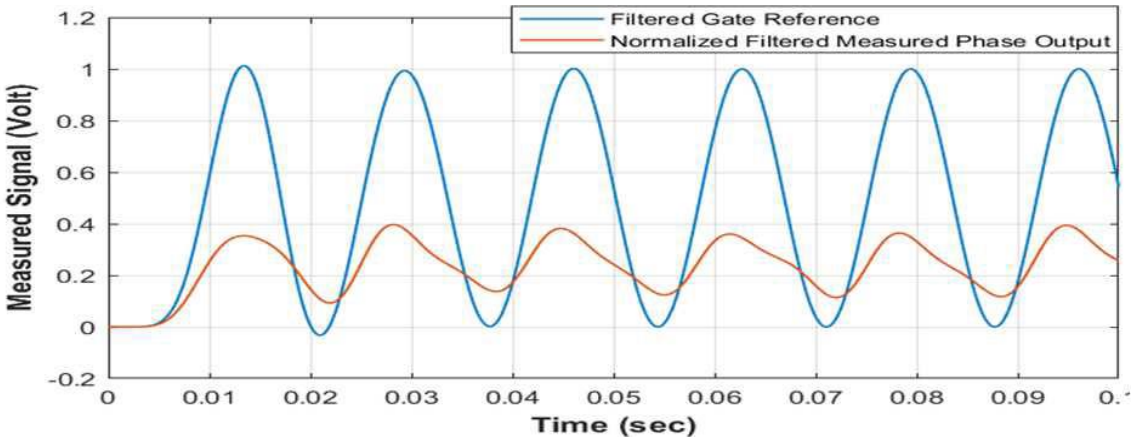

Figure 4.3 The Output and Filtered Reference Waveform – Fault Occurred.

4.2 Simulation of Design In PSIM

To implement the simulation of the design of DC-DC converter, three phase inverter, and PI Control system, PSIM software was used. The relevant circuits, corresponding results and analysis are presented in this section.

4.2.1 Simulation of DC-DC Converter

With a 12 V DC voltage, the desired output voltage is 400 V. To achieve this goal, a design to step up the voltage is required. The DC-DC converter is implemented to boost the voltage up to a much higher value. The simulation parameters are listed in Table 4.3. The topology created in PSIM is as shown in Figure 4.4. As mentioned in the previous chapter, the selected PWM controller is UC3843. The PSIM model of this component is provided in Figure 4.5, where we can see the internally implementation of it. Figure 4.6

shows the output of the DC-DC converter. Pin 6 of this UC3843 controller is connected to the circuit input through the PWM module, so that we can get the PWM modulation waveform in Figure 4.7 to 4.9.

Table 4.3. *Specification of Simulation*

Parameters	Value	Units
Input Voltage	12	V
Output Voltage	400	V

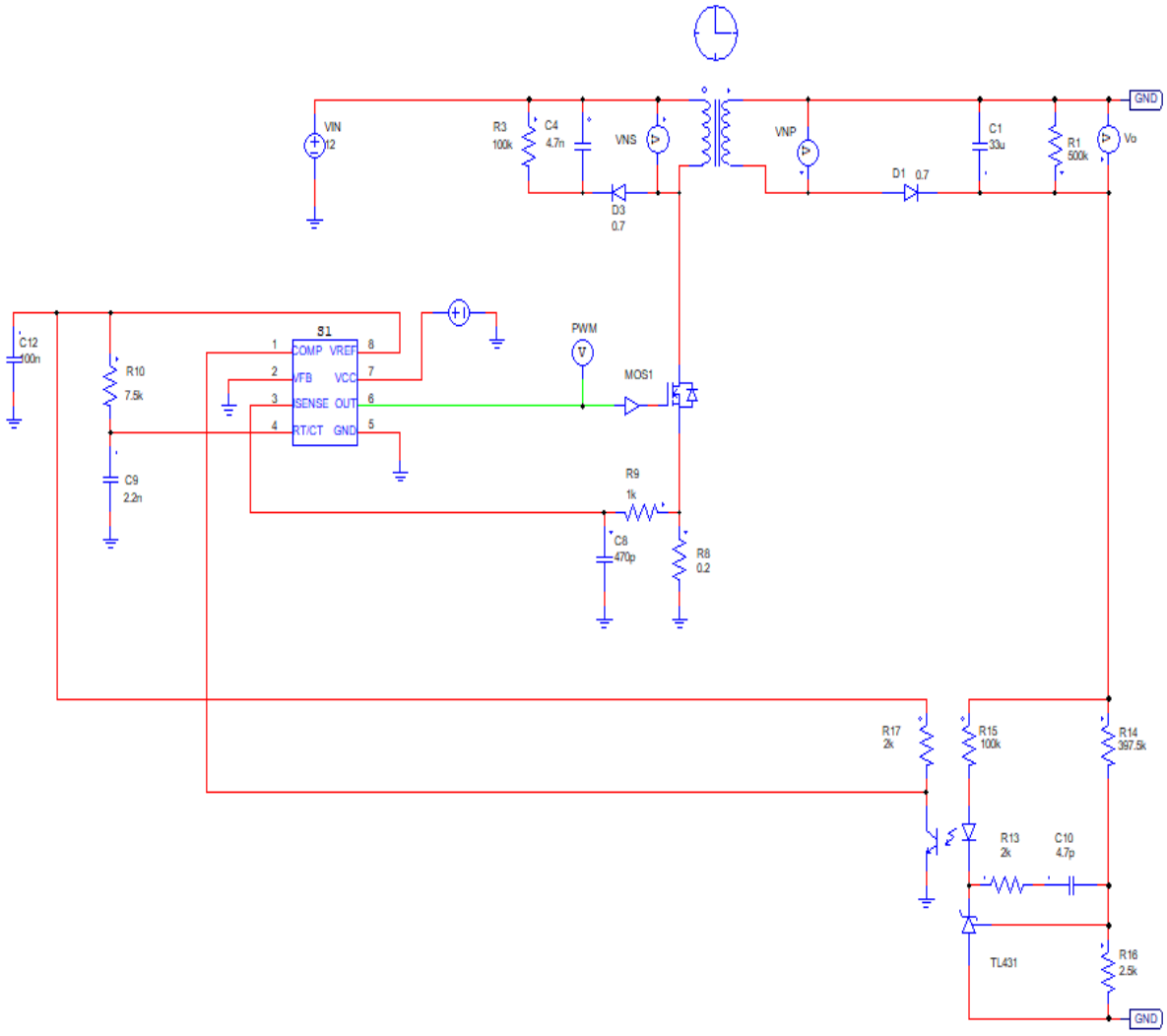

Figure 4.4 DC-DC Converter in PSIM

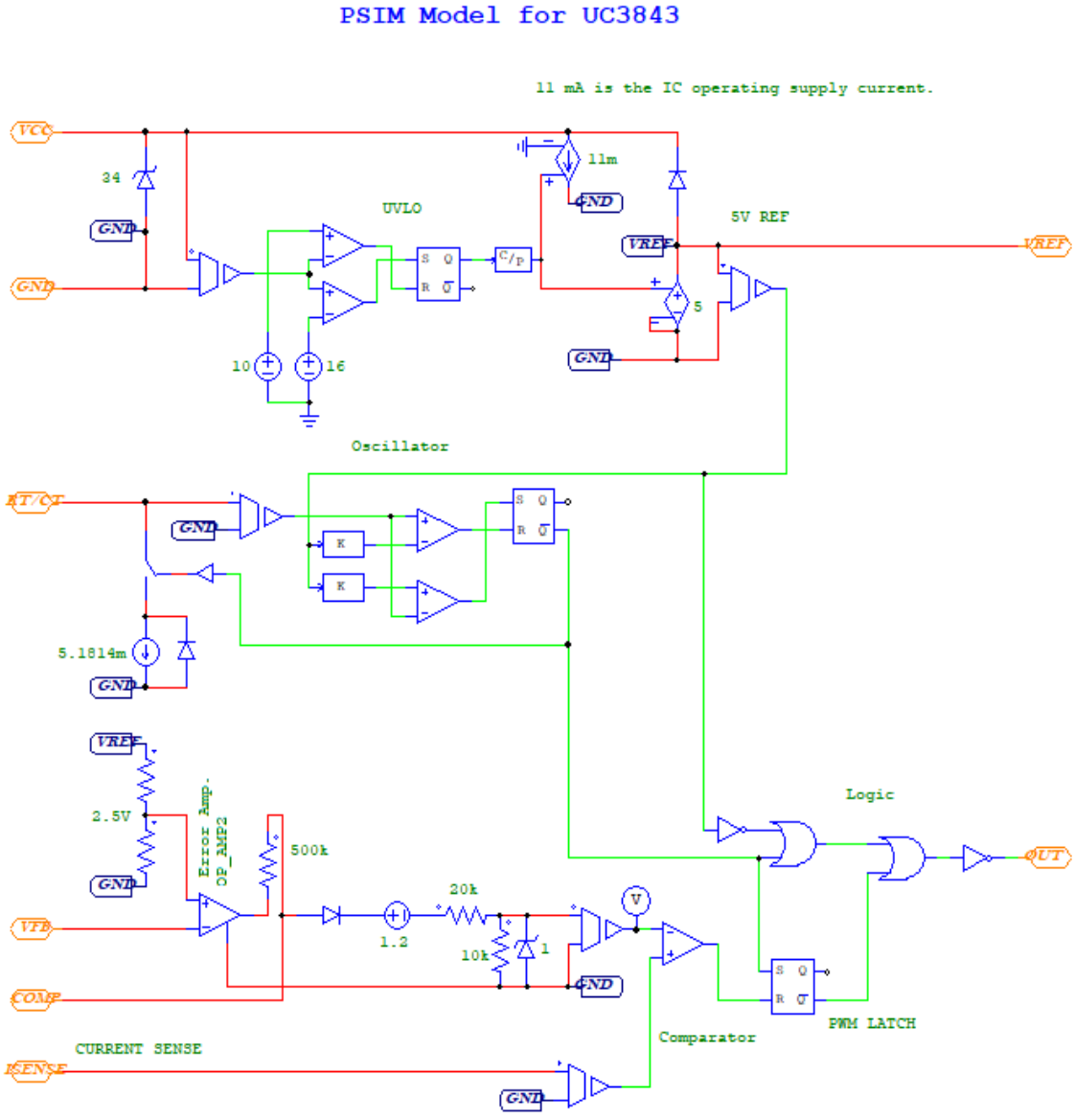

Figure 4.5 PSIM Model for UC3843

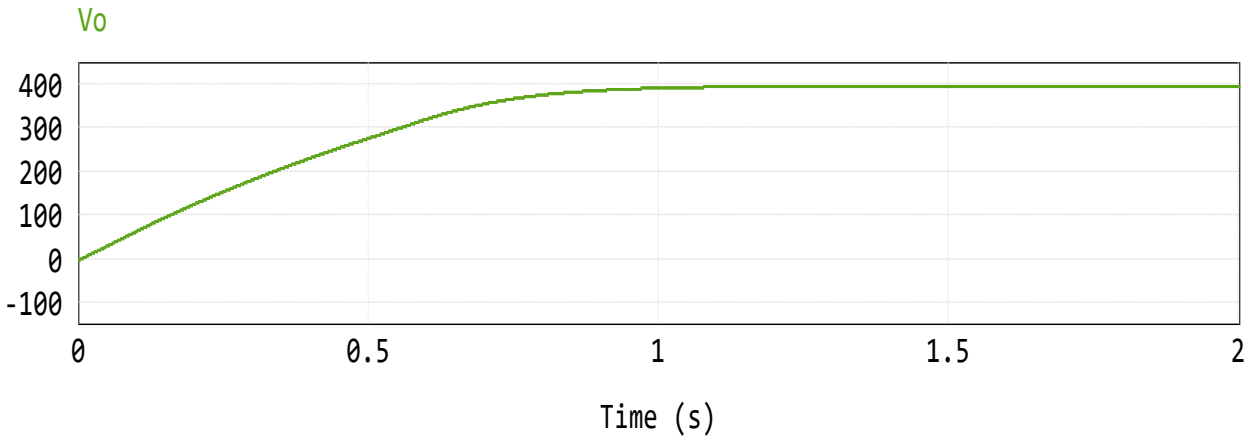

Figure 4.6 Output of the DC-DC Converter

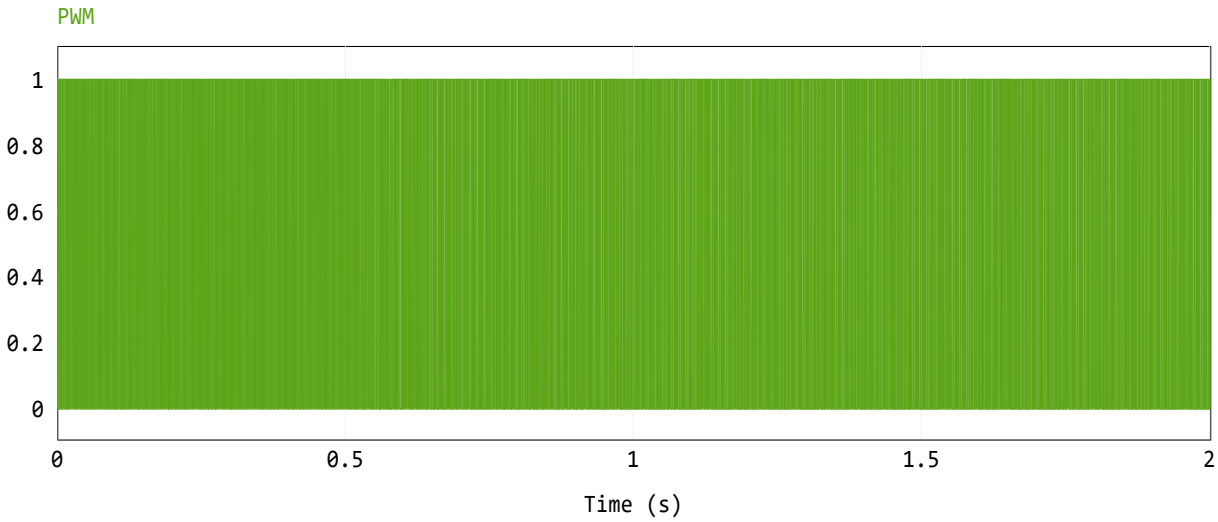

Figure 4.7 PWM Modulation

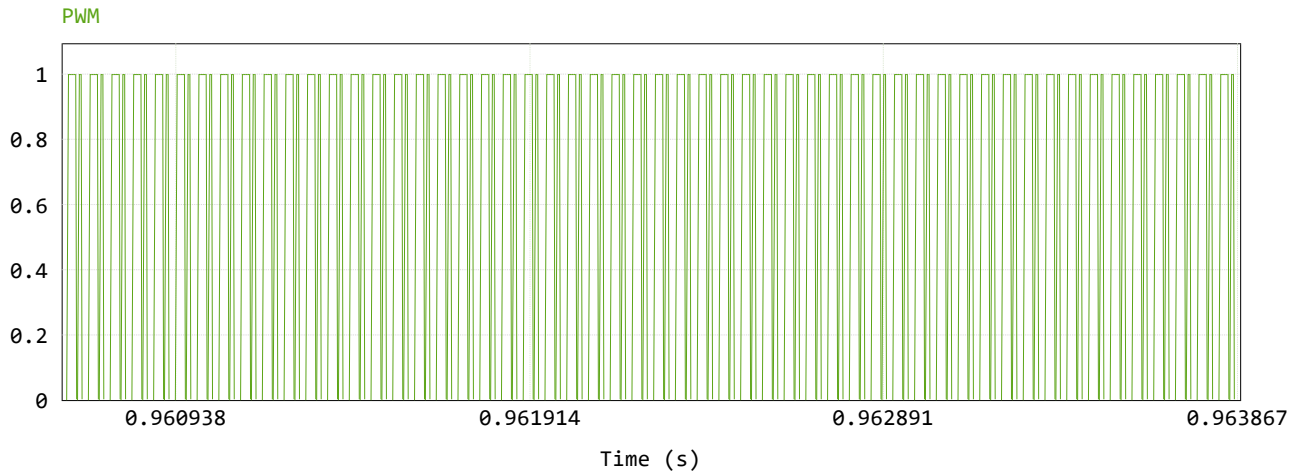

Figure 4.8 PWM Modulation (Zoom in)

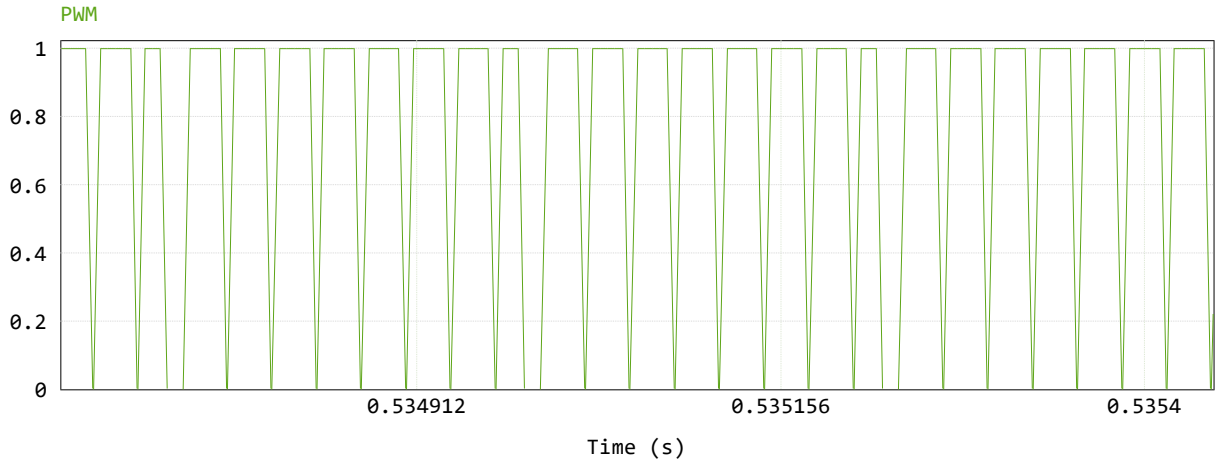

Figure 4.9 PWM Modulation (Zoom in)

4.2.2 Simulation of Three-Phase Inverter

In order to detect the open circuit fault happened in which phase, the bi-directional switches are used. The initial position of the switches is set as closed/open, so that we can

simulate the design to detect and remove the open circuit fault. This section follows steps introduced in [56]. The circuit is setup in PSIM as shown in Figure 4.10. The control algorithm is as indicated in Figure 4.11, the PI control method is applied according to [56].

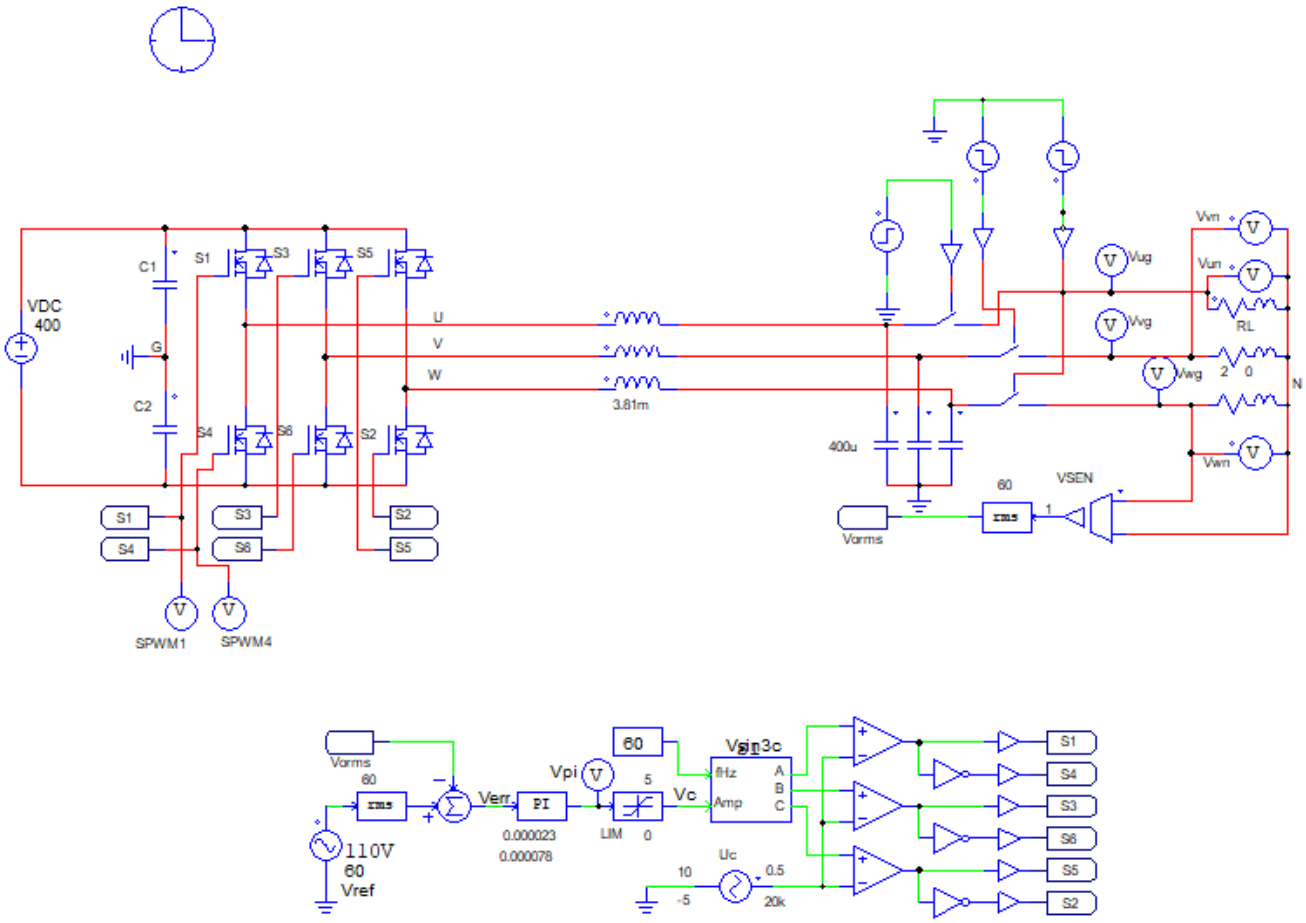

Figure 4.10 Three-Phase Inverter in PSIM

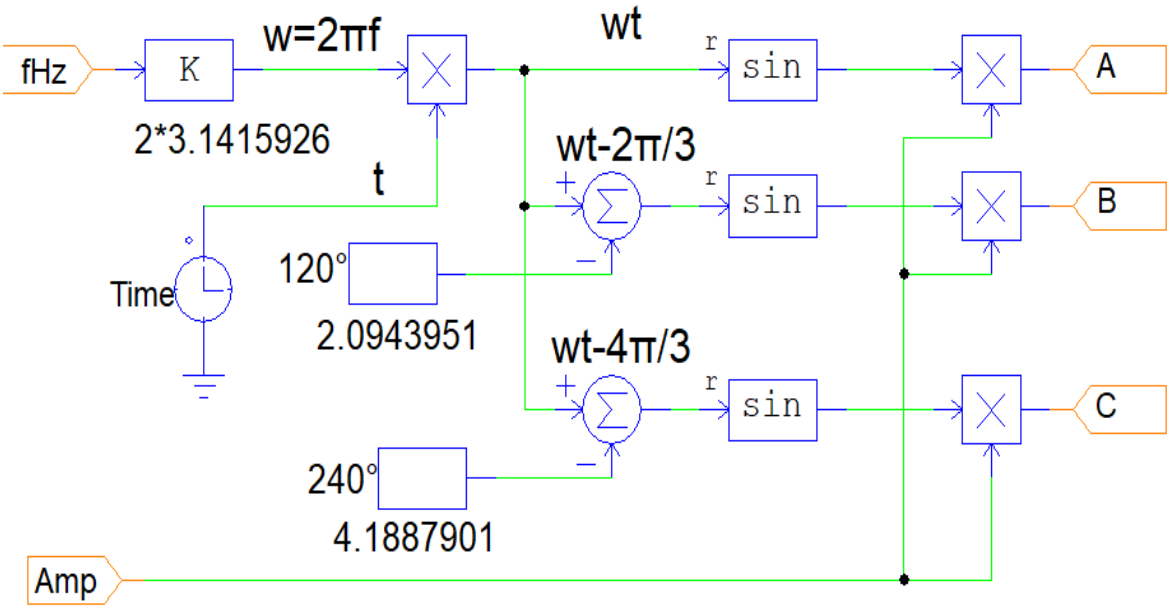

Figure 4.11 PI Control

Figure 4.12 to Figure 4.15 show the simulation results for the three phase separately. All the three phase have detected the open circuit fault at the initial position. In Figure 4.12 and Figure 4.13, at t = 0.1s, phase U and V start to bring the system back to the normal condition. In the end, when t = 0.5s, all the three phase are recovered from the fault, as shown in Figure 4.14. Figure 4.15 is the simulation result with all three phases combined, to provide better visualization.

Figure 4.16 to Figure 4.18 show the closer looks for the simulation results as mentioned earlier, to provide better understanding of the goal of this simulation. In conclusion, the fault is detected and removed successfully by the technique, the inverter will continue work in a healthy condition in the propulsion system.

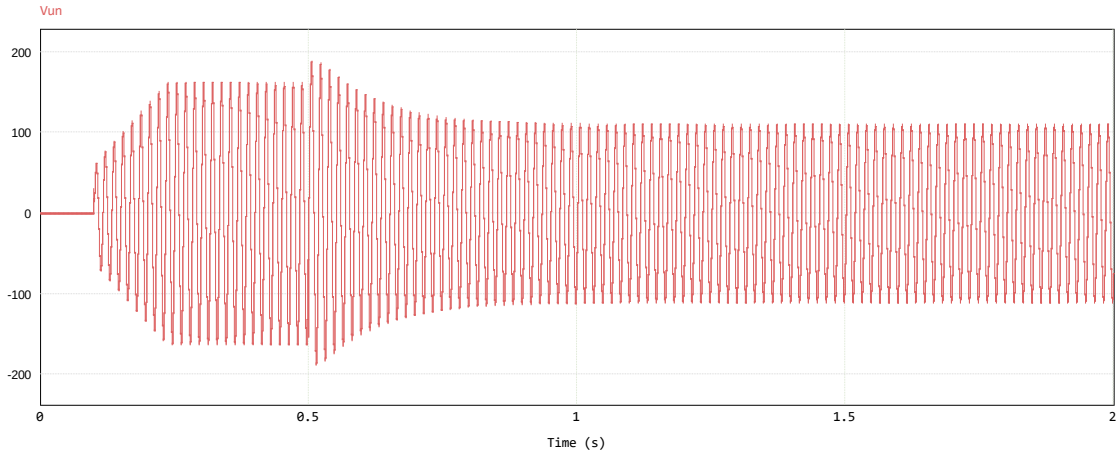

Figure 4.12 Phase-U Simulation Results

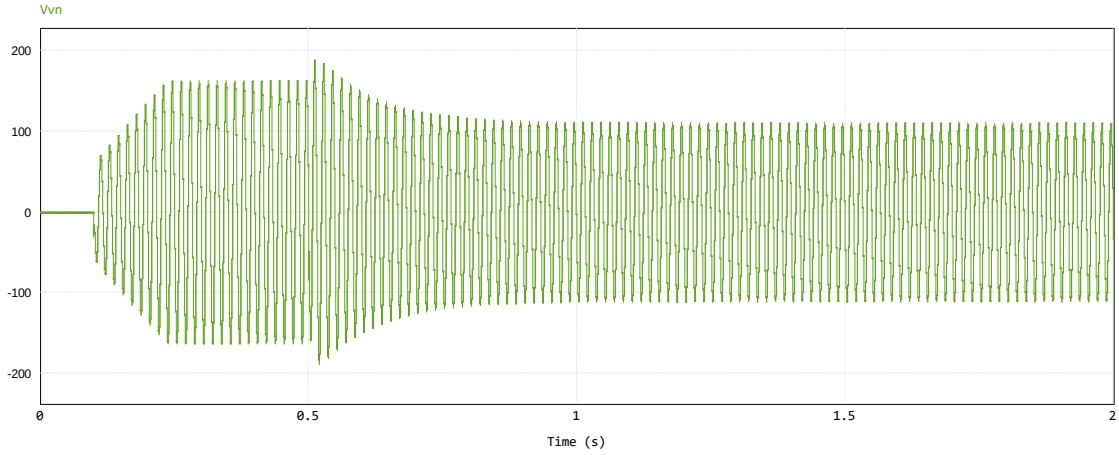

Figure 4.13 Phase-V Simulation Results

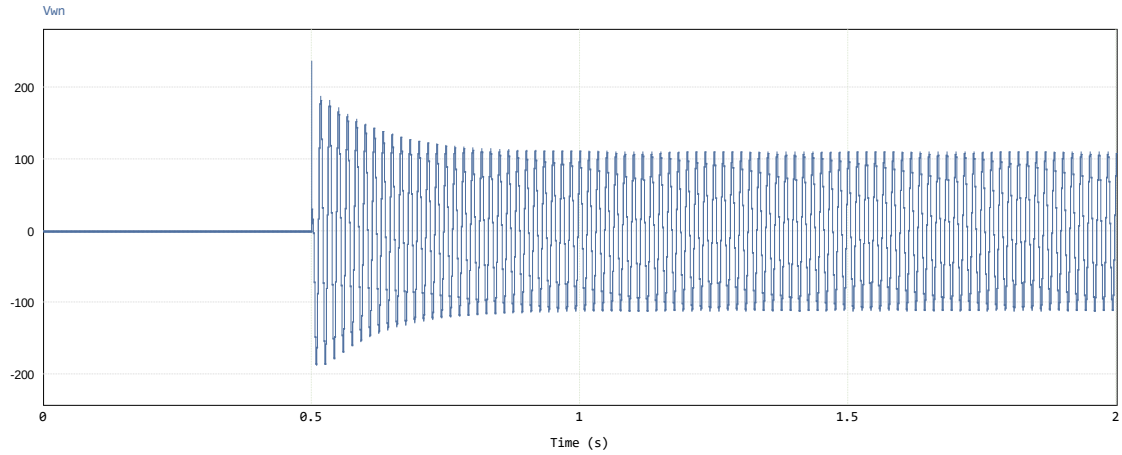

Figure 4.14 Phase-W Simulation Results

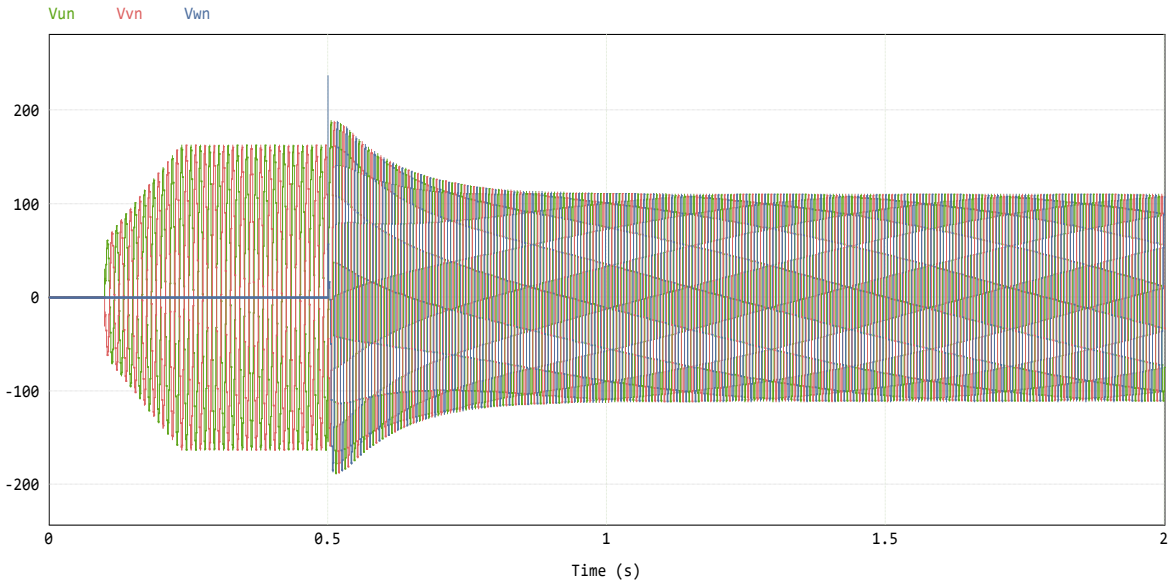

Figure 4.15 Simulation Results

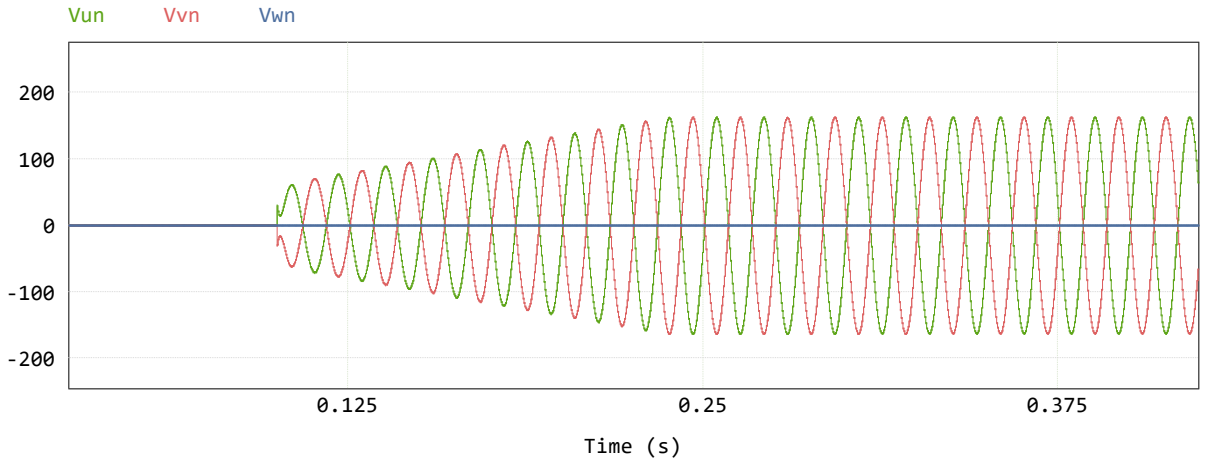

Figure 4.16 Fault Detected in Phase-W

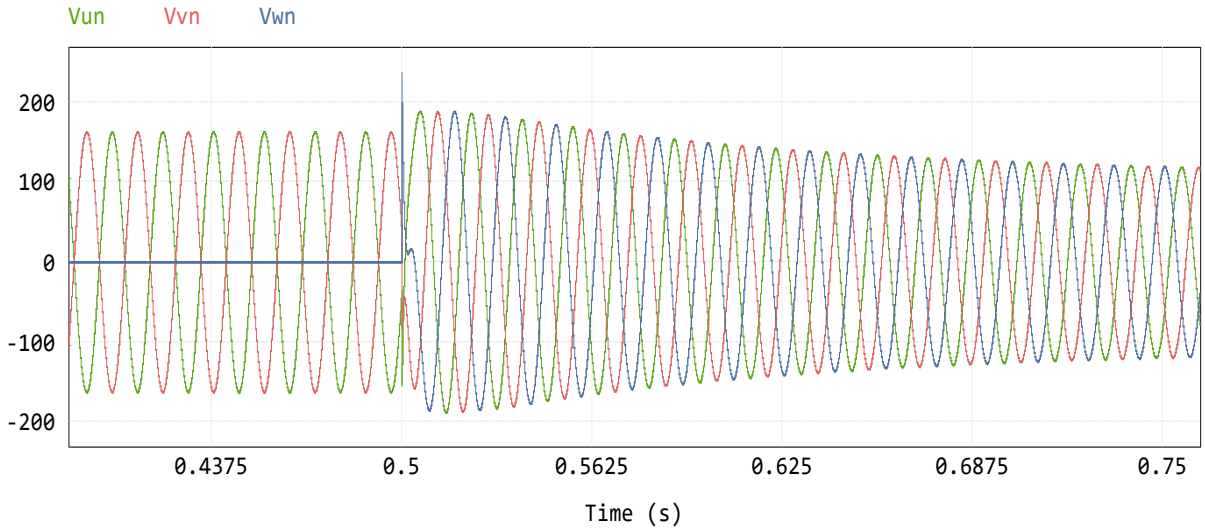

Figure 4.17 Fault Removed

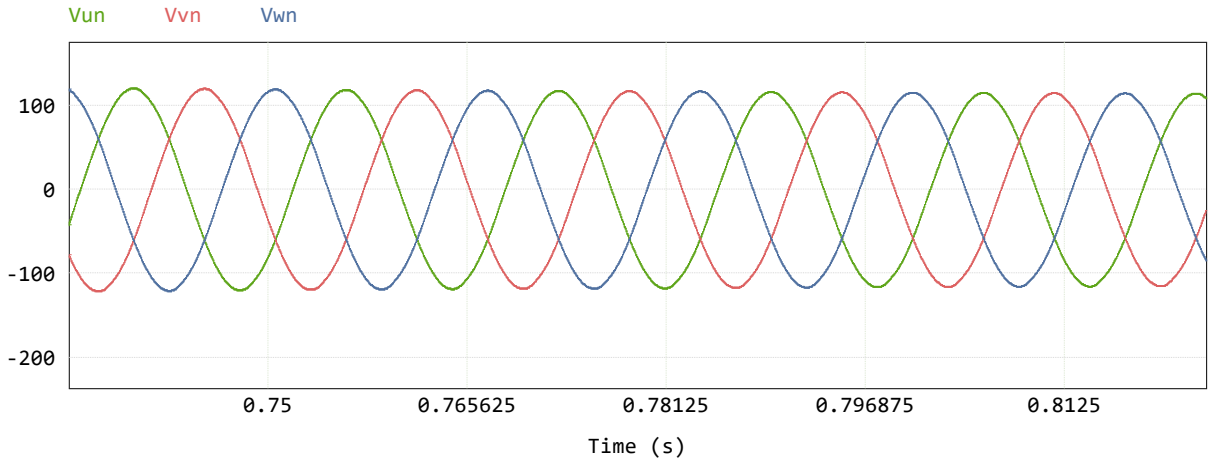

Figure 4.18 Three-Phase Inverter Waveforms

4.3 Experimental Results of Clustering Method

In practical, the open circuit fault of single phase was produced. As shown in the following two figures, the real reference cluster waveforms of the gate driver and the detected output single phase voltage are illustrated. By exporting the data to MATLAB.

The gate and single-phase output in open circuit fault is shown in the pictures. The Figure 4.19(a) shows the output voltage and gate pulse and it gets zoomed in as shown in Figure 4.19(b). Again, these two waveforms are not matched so that we can get the conclusion that the fault is detected in this case.

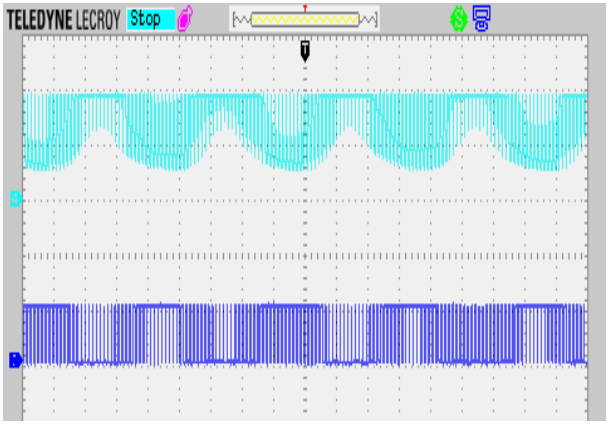

Figure 4.19 (a)

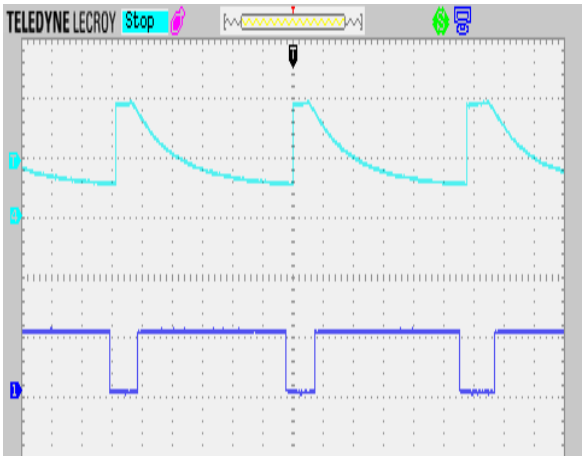

Figure 4.19 (b)

Figure 4.19 Gate and Single-Phase Output in Open Circuit Fault Case

(a) The output voltage and gate pulse

(b) Measurement after zooming

For the no fault case, the light blue line is the measured output signal phase voltage, and the purple line is the measured gate reference. Figure 4.20 (a) shows the gate voltage with the corresponding output waveform and Figure 4.20 (b) is the zoomed in version of the result. We can see that these two measurements are very close to each other, which means there is not fault has occurred.

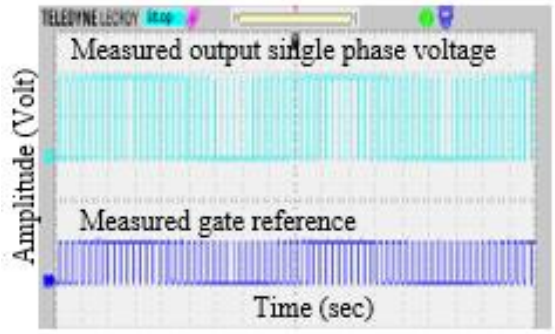

Figure 4.20 (a)

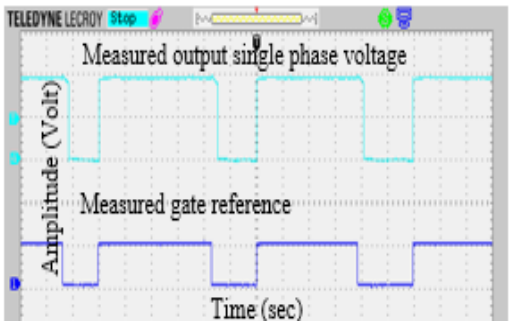

Figure 4.20 (b)

Figure 4.20 Output (single phase) and gate voltage under no fault condition

(a) Gate voltage with the corresponding output waveform

(b) Zoomed measurements

The experiment is implemented by the VSI connected to the water pump motor, which is available in the Power Electronics and Drives Applications Laboratory (PEDAL) of Ontario Tech University. The proposed algorithm is applied to the VSI and used to observe the motor's behavior in healthy and faulty cases, respectively. The equipment of the experiment set up can be seen in the following figures. Figure 4.21(a) has the VSI inside, it is connected to the water pump motor as shown in Figure 4.21(b). A picture of the water

pump for illustration is in Figure 4.21(c). The experimental testing in any power train of a water pump will be similar to that of any electric car, in principle.

(a) (b) (c)

Figure 4.21 VSI; VSI connection to the motor; the water pump motor

Chapter 5. Conclusions and Future Works

5.1 Conclusions

Recently, the industry has shown significant interests in preventing EVs from faults during traveling. This thesis undertakes an extensive exploration of a wide array of fault detection methodologies, providing an in-depth review and thorough discussion of their suitability and potential applications. The core objective centers on the development and implementation of a robust fault diagnosis system tailored specifically for three-phase inverters, a critical component in various electrical systems. This intricate system design involves a painstaking examination of numerous fault scenarios, with the ultimate aim of crafting a versatile and highly effective fault detection strategy. To validate the efficacy of the proposed fault detection approach, a series of intricate simulations are meticulously devised and executed using the PSIM platform. These simulations serve as a rigorous assessment tool, demonstrating the successful identification and subsequent rectification of faults within the inverter system. This research not only contributes to:

- It is the first time this model is built in software like PSIM. Most of the techniques in the literature are hardwired or are with signal processing techniques but requires additional hardware. Our model is based on Artificial Intelligence, no additional hardware or components are required.

- The ongoing evolution of fault detection techniques but also underscores the pragmatic and real-world applicability of the designed fault diagnosis system for three-phase inverters.
- Prior to this work, most of the fault detection system designs are based on signal processing techniques, using the power electronics simulation software – PSIM to carry out such a design is a success.
- This work was verified by the first-hand prototype and the preliminary experimental results are in agreement to provide the proof of concept for that proposed algorithm.

Numerous publications have addressed the subject matter of this thesis, with contributions appearing in esteemed IEEE conferences such as APEC, ECCE, and IEEE ACCESS. Furthermore, a substantial portion of this research has been featured in a specialized journal as part of an invitation extended by CJECE. Additionally, multiple IEEE papers and journals related to this research are currently undergoing the peer review process.

5.2 Future Works

In the future, a more sophisticated laboratory prototype can be built for more testing and experimental results purposes. And more different methodologies can be investigated and implemented to improve the design. The goal is to continuously refine and optimize the fault detection process, and ensure the high level of accuracy, reliability, and real-time responsiveness. This work is regularized and requires a PhD student.

Bibliography

[1] I. Tiseo, “Canada: transportation CO_2 emissions 1970-2021”, *Statista*. 2023

[2] Idaho National Laboratory, “How Do Gasoline & Electric Vehicles Compare?” 2014. [Online]. Available: https://avt.inl.gov/sites/default/files/pdf/fsev/compare.pdf

[3] R. Islam, S. M. S. H. Rafin, and O. A. Mohammed, “Comprehensive Review of Power Electronic Converters in Electric Vehicle Applications,” *Forecasting*. 2022. [Online]. Available: https://doi.org/10.3390/forecast5010002

[4] S. Chakraborty, H.-N. Vu, M. M. Hasan, D.-D. Tran, M. E. Baghdadi, and O. Hegazy, “DC-DC Converter Topologies for Electric Vehicles, Plug-in Hybrid Electric Vehicles and Fast Charging Stations: State of the Art and Future Trends.” *Energies*, 2019. [Online]. Available: https://doi.org/10.3390/en12081569

[5] A. Poorfakhraei, M. Narimani and A. Emadi, "A Review of Modulation and Control Techniques for Multilevel Inverters in Traction Applications," *IEEE Access*, vol. 9, pp. 24187-24204, 2021, doi: 10.1109/ACCESS.2021.3056612.

[6] B. Şarlioğlu, "Automotive Power Electronics: Current Status and Future Trends," 2019 *International Aegean Conference on Electrical Machines and Power Electronics (ACEMP) & 2019 International Conference on Optimization of Electrical and Electronic Equipment (OPTIM)*, Istanbul, Turkey, 2019, pp. 1-2, doi: 10.1109/ACEMP-OPTIM44294.2019.9007120.

[5] E. Nix, “What was the War of the Currents? HISTORY,” 2018, [Online]. Available: https://www.history.com/news/what-was-the-war-of-the-currents

[6] The Authoritative Dictionary of IEEE Standards Terms, Seventh Edition, in IEEE Std 100-2000, vol., no., pp.1-1362, 11 Dec. 2000, doi: 10.1109/IEEESTD.2000.322230.

[7] J. B Andriulli, A. E. Gates, H. D. Haynes, L. B. Klett, S. N. Matthews, E. A. Nawrocki, P. J. Otaduy, M. B. Scudiere, T. J. Theiss, J. F. Thomas, L. M. Tolbert, M. L. Yauss, and C. A. Voltz, “Advanced power generation systems for the 21st Century: Market survey and recommendations for a design philosophy.” 1999, [Online]. Available: Www.osti.gov. https://www.osti.gov/servlets/purl/752077

[8] AG, I. T. (n.d.). “(H)EV traction inverter - hybrid / electric vehicle - Infineon Technologies,” [Online]. Available: Www.infineon.com. Retrieved September 23,

2023, from https://www.infineon.com/cms/en/applications/automotive/electric-drive-train/traction-inverter/

[9] V. Gomathy, and S. Selvaperumal, “Fault Detection and Classification with Optimization Techniques for a Three-Phase Single-Inverter Circuit.” *Journal of Power Electronics*, 2016. *16*(3), 1097–1109. https://doi.org/10.6113/jpe.2016.16.3.1097

[10] B. Gou, X. Ge, S. Wang, X. Feng, J. B. Kuo and T. G. Habetler, "An Open-Switch Fault Diagnosis Method for Single-Phase PWM Rectifier Using a Model-Based Approach in High-Speed Railway Electrical Traction Drive System," in IEEE Transactions on Power Electronics, vol. 31, no. 5, pp. 3816-3826, May 2016, doi: 10.1109/TPEL.2015.2465299.

[11] J. A. Reyes-Malanche, F. J. Villalobos-Pina, E. Cabal-Yepez, R. Alvarez-Salas and C. Rodriguez-Donate, "Open-Circuit Fault Diagnosis in Power Inverters Through Currents Analysis in Time Domain," in IEEE Transactions on Instrumentation and Measurement, vol. 70, pp. 1-12, 2021, Art no. 3517512, doi: 10.1109/TIM.2021.3082325.

[12] S. Madichetty, S. Mishra, and M. Basu, “New trends in electric motors and selection for electric vehicle propulsion systems,” *IET Electr. Syst. Transp*. 2021. vol. 11, no. 3, pp. 186–199,

[13] S. Eriksson, “Permanent magnet synchronous machines,” *Energies*, 2019.vol. 12, no. 14,

[14] Y. Chen, S. Liang, W. Li, H. Liang, and C. Wang, “Faults and diagnosis methods of permanent magnet synchronous motors: A review,” 2019Appl. Sci., vol. 9, no. 10.

[15] G. Selvaraj, A. R. Sadat, H. S. Krishnamoorthy, and K. Rajashekara, “An Improved Fault-Tolerant Power Converter for Electric Vehicle Propulsion,” *2020 IEEE Int. Conf. Power Electron. Smart Grid Renew. Energy, PESGRE* 2020, pp. 1–5, 2020.

[16] M. Ibrahim, A. Rassõlkin, T. Vaimann, and A. Kallaste, “Overview on Digital Twin for Autonomous Electrical Vehicles Propulsion Drive System,” 2022.Sustain., vol. 14, no. 2

[17] C. S. Wang, I. H. Kao, and J. W. Perng, “Fault diagnosis and fault frequency determination of permanent magnet synchronous motor based on deep learning,” *Sensors*, 2021vol. 21, no. 11.

[18] T. Roubache, S. Chaouch, and M. S. Naït-Saïd, “Backstepping design for fault detection and FTC of an induction motor drives-based EVs,” *Automatika,* 2017. vol. 57, no. 3, pp. 736–748

[19] J. Zhang, M. Salman, W. Zanardelli, S. Ballal, and B. Cao, “An Integrated Fault Isolation and Prognosis Method for Electric Drive Systems of Battery Electric Vehicles,” *IEEE Trans. Transp. Electrif,* 2021.vol. 7, no. 1, pp. 317–328.

[20] G. Rigatos, N. Zervos, M. Abbaszadeh, P. Siano, D. Serpanos, and V. Siadimas, “Neural networks and statistical decision making for fault diagnosis of PM linear synchronous machines,” Int. J. Syst. Sci., 2020. vol. 51, no. 12, pp. 2150–2166.

[21] D. C. Robertson, O. I. Camps, J. S. Mayer and W. B. Gish, "Wavelets and electromagnetic power system transients," in *IEEE Transactions on Power Delivery*, vol. 11, no. 2, pp. 1050-1058, April 1996, doi: 10.1109/61.489367.

[22] Z. German-Sallo, G. Strnad, “Signal Processing Methods in Fault Detection in Manufacturing Systems,” 11th International Conference Interdisciplinarity in Engineering, 2017.

[23] V. Shankar, A. Kumar and A. N. Tiwari, "Performance Analysis of Three Phase Voltage Source Inverter using PWM and SPWM Techniques," *2019 International Conference on Computing, Power and Communication Technologies (GUCON)*, New Delhi, India, 2019, pp. 759-763.

[24] N. M. Kolmakov and I. A. Bakhovtsev, "Three-phase current source inverter with hysteresis control in voltage source mode," *2015 16th International Conference of Young Specialists on Micro/Nanotechnologies and Electron Devices*, Erlagol, Russia, 2015, pp. 429-432, doi: 10.1109/EDM.2015.7184577.

[25] P. Krause, O. Wasynczuk, S. Sudhoff, and S. Pekarek, *Analysis of Electric Machinery and Drive Systems*. 2013.

[26] M. Vujacic, M. Hammami, M. Srndovic and G. Grandi, "Evaluation of DC voltage ripple in three-phase PWM voltage source inverters," *2017 IEEE 26th International Symposium on Industrial Electronics (ISIE)*, Edinburgh, UK, 2017, pp. 711-716, doi: 10.1109/ISIE.2017.8001333.

[27] N. Lopatkin, "PSIM Model of Quarter-Wave Symmetric Space Vector PWM Modulator for Three-Phase Multilevel Voltage Source Inverter," *2020 Ural Symposium on Biomedical Engineering, Radioelectronics and Information*

Technology (USBEREIT), Yekaterinburg, Russia, 2020, pp. 0309-0312, doi: 10.1109/USBEREIT48449.2020.9117616.

[28] J. Lee and J. -W. Park, "PWM Selection Method for High Performance of Two-Level Three-Phase Voltage Source Inverters in High Load Power Factor Ranges," *2021 IEEE 12th Energy Conversion Congress & Exposition - Asia (ECCE-Asia), Singapore, Singapore, 2021*, pp. 682-687, doi: 10.1109/ECCE-Asia49820.2021.9479252.

[29] M. Vujacic, M. Hammami, M. Srndovic and G. Grandi, "Evaluation of DC voltage ripple in three-phase PWM voltage source inverters," *2017 IEEE 26th International Symposium on Industrial Electronics (ISIE)*, Edinburgh, UK, 2017, pp. 711-716, doi: 10.1109/ISIE.2017.8001333.

[30] N. N. Lopatkin, "Voltage source multilevel inverter voltage quality comparison under multicarrier sinusoidal PWM and space vector PWM of two delta voltages," *2017 International Multi-Conference on Engineering, Computer and Information Sciences (SIBIRCON)*, Novosibirsk, Russia, 2017, pp. 439-444, doi: 10.1109/SIBIRCON.2017.8109923.

[31] T. Zhao, Q. Zong, T. Zhang and Y. Xu, "Study of photovoltaic three-phase grid-connected inverter based on the grid voltage-oriented control," *2016 IEEE 11th Conference on Industrial Electronics and Applications (ICIEA)*, Hefei, China, 2016, pp. 2055-2060, doi: 10.1109/ICIEA.2016.7603927.

[32] K. S. A. Algarny, M. Vilathgamuwa, M. Broadmeadow and W. Choi, "Independent Voltage Oriented DC-Side Sensorless Control of Three-Phase Cascaded H-bridge Multilevel Inverter With Decentralized MPPTs," *2020 IEEE 29th International Symposium on Industrial Electronics (ISIE)*, Delft, Netherlands, 2020, pp. 740-743, doi: 10.1109/ISIE45063.2020.9152267.

[33] S. A. Zulkifli, "Voltage oriented controller using dual loops control for power flow in distributed generation network," *2015 10th Asian Control Conference (ASCC), Kota Kinabalu*, Malaysia, 2015, pp. 1-7, doi: 10.1109/ASCC.2015.7244797.

[34] F. TLILI and F. BACHA, "Comparative Study of Control Strategies for Three Phase Bidirectional AC/DC Converter," *2023 IEEE International Conference on Advanced Systems and Emergent Technologies (IC_ASET)*, Hammamet, Tunisia, 2023, pp. 1-6, doi: 10.1109/IC_ASET58101.2023.10150692.

[35] R. M. Kennel, M. Linke and P. Szczupak, ""Sensorless" control of 4-quadrant-rectifiers for voltage source inverters (VSI)," *IEEE 34th Annual Conference on Power Electronics Specialist*, 2003. PESC '03., Acapulco, Mexico, 2003, pp. 1057-1062 vol.3, doi: 10.1109/PESC.2003.1216596.

[36] M. Alathamneh, H. Ghanayem and R. M. Nelms, "Power Control of a Three-phase Grid-connected Inverter using a PI Controller under Unbalanced Conditions," SoutheastCon 2022, Mobile, AL, USA, 2022, pp. 447-452, doi: 10.1109/SoutheastCon48659.2022.9764097.

[37] A. Cherifi, A. Chouder, A. Kessal, A. Hadjkaddour, A. Aillane and K. Louassaa, "Control of a Voltage Source Inverter in a Microgrid Architecture using PI and PR Controllers," *2022 19th International Multi-Conference on Systems, Signals & Devices (SSD)*, Sétif, Algeria, 2022, pp. 1471-1477, doi: 10.1109/SSD54932.2022.9955891.

[38] G. Sun and X. Hu, "An Enhanced Control Strategy for Three-phase ZVR Grid-Connected Inverter Under Unbalanced and Distorted Grid Voltage Conditions," *2019 Chinese Control Conference (CCC)*, Guangzhou, China, 2019, pp. 7448-7453, doi: 10.23919/ChiCC.2019.8865831.

[39] S. Bhowmik, P. K. Gayen and A. Mitra, "Performance Comparison between PI based Control and Model Predictive Control of Voltage Source Inverter under Load Variations," *2022 IEEE International Conference of Electron Devices Society Kolkata Chapter (EDKCON)*, Kolkata, India, 2022, pp. 344-348, doi: 10.1109/EDKCON56221.2022.10032916.

[40] Ma Liang and T. Q. Zheng, "Synchronous PI control for three-phase grid-connected photovoltaic inverter," *2010 Chinese Control and Decision Conference, Xuzhou, China, 2010*, pp. 2302-2307, doi: 10.1109/CCDC.2010.5498813.

[41] O. A. Vavilov, V. D. Yurkevich and D. V. Korobkov, "Resonant PI-Controller Design Based on the Time-Scale Separation Method for a Two-Level Voltage Inverter," *2022 IEEE International Multi-Conference on Engineering, Computer and Information Sciences (SIBIRCON)*, Yekaterinburg, Russian Federation, 2022, pp. 1360-1364, doi: 10.1109/SIBIRCON56155.2022.10017064.

[42] G. Tsengenes and G. Adamidis, "Comparative evaluation of Fuzzy-PI and PI control methods for a three-phase grid connected inverter," *Proceedings of the 2011 14th European Conference on Power Electronics and Applications*, Birmingham, UK, 2011, pp. 1-10.

[45] B. M. Wilamowski and J. D. Irwin, *The Industrial Electronics Handbook: Power Electronics and Motor Drives*. 2011.

[43] V. Shankar, A. Kumar and A. N. Tiwari, "Performance Analysis of Three Phase Voltage Source Inverter using PWM and SPWM Techniques," 2019 International Conference on Computing, Power and Communication Technologies (GUCON), New Delhi, India, 2019, pp. 759-763.

[44] W. Ahmed, and S. M. U. Ali, "Comparative study of SVPWM (space vector pulse width modulation) & SPWM (sinusoidal pulse width modulation) based three phase voltage source inverters for variable speed drive." *IOP Conference Series: Materials Science and Engineering*, 2013, [Online] Available: https://doi.org/10.1088/1757-899x/51/1/012027

[45] B. M. Wilamowski and J. D. Irwin, *The Industrial Electronics Handbook: Power Electronics and Motor Drives*. 2011.

[46] X, Tao. "*Selection and calculation of switching power supply RCD circuit parameters*,"2012.

[47] X, Tao. "Principle of switching power supply," 2012.

[48] Altium. *PWM in Power Supply Design*. (2021, November 5). [Online] Available: https://resources.altium.com/p/pwm-power-supply-design

[49] Mouser Electronics, "UC3842/UC3843/UC3844/UC3845 SMPS Controller."

[50] Refa Electronics, "Fixed Frequency Current Mode PWM Controller," 2008.

[51] S. Yin, Y. Gu, S. Deng, X. Xin, and G. Dai, "Comparative investigation of surge current capabilities of Si IGBT and SiC MOSFET for pulsed power application," IEEE Transactions on Plasma Science, vol. 46, no. 8, pp. 2979–2984, Aug. 2018.

[52] T. Van Nguyen, P. Jeannin, E. Vagnon, D. Frey, and J. Crebier, "Series connection of IGBTs with self-powering technique and 3-D topology," IEEE Transactions on Industry Applications, vol. 47, no. 4, pp. 1844– 1852, Jul. 2011.

[53] N. Anurag and S. Nath, "Effect of Optocoupler Gate Drivers on SiC MOSFET," 2021 National Power Electronics Conference (NPEC), Bhubaneswar, India, 2021, pp. 01-06, doi: 10.1109/NPEC52100.2021.9672531.

[54] “Optocoupler Circuit Design and Detailed Analysis” Electronics Believer, Apr. 2015.

[55] N. Muhammad H. Rashid Kumar and A. R. Ashish R. Kulkarni, “Power electronics: devices, circuits and applications,” p. 1022, 2014.

[56] Z. You, F. Dai, Z. Zhang, C. Bian, *PSIM Simulation and Application of Power Electronics*. 2020.